Ba distribution in surface Southern Ocean sediments and export production estimates

Nathalie Fagel,[1] Frank Dehairs,[2] Luc André,[3] Gilles Bareille,[4,5] and Christophe Monnin[6]

[1]   We present excess Ba (Baxs) data (i.e., total Ba corrected for lithogenic Ba) for surface sediments from a north-south transect between the Polar Front Zone and the northern Weddell Gyre in the Atlantic sector and between the Polar Front Zone and the Antarctic continent in the Indian sector. Focus is on two different processes that affect excess Ba accumulation in the sediments: sediment redistribution and excess Ba dissolution. The effect of these processes needs to be corrected for in order to convert accumulation rate into vertical rain rate, the flux component that can be linked to export production. In the Southern Ocean a major process affecting Ba accumulation rate is sediment focusing, which is corrected for using excess ^{230}Th. This correction, however, may not always be straightforward because of boundary scavenging effects. A further major process affecting excess Ba accumulation is barite dissolution during exposure at the sediment-water column interface. Export production estimates derived from excess ^{230}Th and barite dissolution corrected Baxs accumulation rates (i.e., excess Ba vertical rain rates) are of the same magnitude but generally larger than export production estimates based on water column proxies (^{234}Th-deficit in the upper water column; particulate excess Ba enrichment in the mesopelagic water column). We believe export production values based on excess Ba vertical rain rate might be overestimated due to inaccurate assessment of the Baxs preservation rate. Barite dissolution has, in general, been taken into account by relating it to exposure time before burial depending on the rate of sediment accumulation. However, the observed decrease of excess Ba content with increasing water column depth (or increasing hydrostatic pressure) illustrates the dependence of barite preservation on degree of saturation in the deep water column in accordance with available thermodynamic data. Therefore correction for barite dissolution would not be appropriate by considering only exposure time of the barite to some uniformly undersaturated deep water but requires also that regional differences in degree of undersatuation be taken into account.   INDEX TERMS: 1050 Geochemistry: Marine geochemistry (4835, 4850); 4835 Oceanography: Biological and Chemical: Inorganic marine chemistry; KEYWORDS: excess Ba, sediment, Southern Ocean, export production

1.   Introduction

[2]   Numerous studies have emphasized the importance of the Southern Ocean in regulating atmospheric carbon dioxide content [*Knox and McElroy*, 1984; *Sarmiento and Toggweiler*, 1984; *Siegenthaler and Wenk*, 1984; *Broecker and Peng*, 1989; *Keir*, 1990; *Martin et al.*, 1990; *Shemesh et al.*, 1993; *Moore et al.*, 2000; *Stephens and Keeling*, 2000]. Spatiotemporal variability of oceanic primary production and related export of organic carbon to the deep sea and the sediment were invoked as major mechanisms explaining variations of the atmospheric carbon dioxide level between glacial and interglacial Pleistocene stages [e.g., *Sarmiento and Toggweiler*, 1984; *Martin et al.*, 1990; *Keir*, 1990]. Controversial hypotheses were advanced, in favor [e.g., *Martin*, 1990; *Kumar et al.*, 1993] or against an increased productivity during glacial periods in the Southern Ocean [e.g., *François et al.*, 1992,

1997; *Bareille et al.*, 1998; *Frank et al.*, 2000]. This controversy is linked partly to the different geochemical behavior of the proxies used to reconstruct past export production. Sedimentary barite is, or is supposed to be, one of the most promising proxies. A correlation between biological productivity in surface waters and Ba, or barite content, was evidenced in recent and past marine sediments [*Goldberg and Arrhenius*, 1958; *Church*, 1979; *Schmitz*, 1987; *Shimmield*, 1992; *Von Breymann et al.*, 1992; *Gingele and Dahmke*, 1994; *Frank et al.*, 1996; *Paytan et al.*, 1996; *Nürnberg et al.*, 1997]. Studies of the water column related the abundance of suspended particulate Ba (especially composed of barite microcrystals) to plankton activity and more precisely to the breakdown of plankton detritus [*Dehairs et al.*, 1980, 1997; *Bishop*, 1988]. This link was evidenced in the Southern Ocean by the symmetric evolution of particulate Ba and dissolved oxygen profiles and pCO$_2$ with water depth [*Dehairs et al.*, 1991; *Stroobants et al.*, 1991]. These different observations suggest that barite is a suitable proxy for export production [*Dymond et al.*, 1992; *Paytan et al.*, 1996; *Shimmield et al.*, 1994; *François et al.*, 1995; *Nürnberg et al.*, 1997].

[3]   A widely applied method for assessing export production requires the measurement of total sedimentary barium content. The excess Ba (Baxs) content, which is assumed to consist mainly of biogenic barite, is estimated by correcting for Ba of detrital origin. Baxs is only an estimate of the effective sedimentary barite content. Selective leachings on Pacific sediment trap samples emphasize that up to 50% of the Baxs might not be barite but rather Ba adsorbed or bound on organic matter and carbonates [*Dymond et al.*, 1992]. According to *Schroeder et al.* [1997] this nonbarite Baxs results from dissolved Ba being scavenged by settling particles in the water column. At the sediment-water interface, such particles would be affected by early diagenesis with subse-

^{1}Clay Mineralogy Department, Université de Liège, Liège, Belgium.
^{2}Analytical Chemistry Department, Vrije Universiteit Brussel, Brussels, Belgium.
^{3}Mineralogy and Geochemistry Department, Royal Museum for Central Africa, Tervuren, Belgium.
^{4}Geology and Oceanography Department, University of Bordeaux, Bordeaux, France.
^{5}Laboratoire de Chimie Analytique Bio-organique et Environnement (LCABIE), UMR-CNRS 5034, Université de Pau et des Pays de l'Adour, Pau, France.
^{6}Laboratory of Geochemistry, University Paul Sabatier, Toulouse, France.

quent transfer of Ba to Fe oxide components of the sediments. In certain situations the use of the barite phase rather than total Baxs should be the preferred proxy tool [*Schroeder et al.*, 1997]. Using a sequential leaching procedure [*Paytan et al.*, 1993], *Paytan et al.* [1996] extracted the barite fraction from a few grams of Pacific sediment and estimated the barite accumulation rate. This rate was subsequently converted to primary production. However, the efficiency of leaching experiments on barite separation is difficult to control [*Cardinal et al.*, 1999; D. Cardinal, personal communication, 2000], and in many cases the amount of sample is insufficient for a sequential leaching.

[4] Different algorithms have been proposed to quantify export production from Baxs. These algorithms reflect primarily the link between export production and particulate organic carbon (POC) flux in the deep sea (e.g., *Sarnthein et al.* [1988]; see also *Bishop* [1989] for a review). POC flux was subsequently substituted for Baxs flux on the basis of the vertical evolution of POC/Baxs ratio in particulate matter sinking through the water column [*Dymond et al.*, 1992; *François et al.*, 1995; *Frank*, 1996; *Nürnberg et al.*, 1997], a procedure linking Baxs flux in the water column or Baxs flux arriving at the sediments (vertical rain rate (VRR)) to export production. The situation is, however, complicated in that the POC/Baxs evolution through the water column has been proposed to depend on sampling depth and on dissolved Ba content in intermediate and deep waters [*Dymond et al.*, 1992] or on sampling depth only [*François et al.*, 1995].

[5] In the present study, we report the latitudinal distribution of Baxs in sediments underlying different hydrodynamic entities of the Atlantic and Indian sectors in the Southern Ocean, characterized by different present-day productivity levels. The discussion will focus on the corrections that have to be applied to reconstruct export productivity from sediment Baxs.

2. Site Description

[6] The positions of the circumpolar frontal systems are determined by the different flow regimes of the Antarctic Circumpolar Current [*Orsi et al.*, 1995]. The main current jets within the eastward flowing Antarctic Circumpolar Current are associated with the Subantarctic Front and the Polar Front. For the Atlantic sector a third frontal system, farther south, coincides with the Antarctic Circumpolar Current-Weddell Gyre Boundary [*Peterson and Stramma*, 1991; *Smetacek et al.*, 1997]. For the Atlantic sector the sampled areas covered the Polar Front Zone (PFZ) and the Antarctic Zone. The former zone extends between the Subantarctic Front and the Polar Front and is characterized by large mesoscale variability due to meandering of the fronts and to eddy formation [*Veth et al.*, 1997]. The Antarctic Zone represents the region between the southern edge of the Polar Front and the northern limit of the Weddell Gyre. For the Indian sector the sampled areas covered the Subantarctic Zone (SAZ; i.e., the region between the Subtropical Front and the Subantarctic Front), the PFZ, and the Antarctic Zone, with the latter representing the region between Polar Front and Antarctic slope. The Antarctic Zone can, in general, be subdivided into a permanent ice-free zone (permanently open ocean zone, or POOZ) and a seasonal ice zone (SIZ).

[7] In the Atlantic sector, 14 box core samples (Figure 1a and Table 1) were recovered during R/V *Polarstern* cruise ANT X/6 (October–November 1992) between 46° and 58°S along 6°W [*Bathmann et al.*, 1997]. This transect crossed the Polar Front Zone, the Antarctic Zone, and the Antarctic Circumpolar Current-Weddell Gyre Boundary, south of 58°S [*Veth et al.*, 1997]. A fourth frontal system, the Southern Polar Front, was identified close to 56°45′S and coincided with the axis of the America-Antarctic Ridge [*Veth et al.*, 1997]. During the ANT X/6 cruise the maximal winter extent of the sea ice cover reached 55°S. The biomass and

primary productivity remained low and constant (<0.2 μg Chl *a* and 80–260 mg C m^{-2} d^{-1}, respectively) during October–November in the ice-free Antarctic Zone. In contrast, the region influenced by the meandering of the Polar Front had a high primary productivity (up to 2900 mg C m^{-2} d^{-1}) [*Bathmann et al.*, 1997] with a large contribution of diatoms [*Quéguiner et al.*, 1997]. Smear slide observations showed that the main sediment components were diatoms, foraminifera, detrital grains, clay aggregates, and accessory volcanic glasses. The sediments were dominated by diatomaceous muds, except for three foraminifera-dominated samples (PS2374, PS2372, and PS2364).

[8] For the Indian sector (Figure 1b) we analyzed 35 box core and Kullenberg core samples from the area between the Subantarctic Front and the Antarctic slope (between 44.7° and 65°S, Table 2), collected during the French APSARA cruises (R/V *Marion Dufresne* [*Bareille*, 1991; *Bareille et al.*, 1991]). The plankton communities in surface waters are dominated by calcium carbonate-secreting plankton in the Subtropical and Subantarctic Zones, while diatoms dominate the community south of the Polar Front [*Bareille et al.*, 1998]. The lithology of the sediments reflects this distribution, with foraminiferal oozes in the northern part of the transect and diatomaceous oozes south of the Polar Front.

3. Methods

[9] Al was analyzed by inductively coupled plasma-atomic emission spectrometry (ICP-AES; ARL 35000C) on an alkaline fusion (lithium metaborate, Baker, Reagent Grade) of 100 mg of dry homogenized sediment. An artificial standard solution (Titrisol-Merck) was used for calibration. Accuracy, determined using international standard reference rocks, was 10% [*Navez*, 1985].

[10] For other elements (Ti, Ca, Sr, Zr, Ba, Nd, and Th) the sediment was digested in a Teflon bomb using concentrated acids (4 g HF and 1g HNO$_3$). Teflon bombs were left under pressure at 180°C for three nights. After adding 1.5 g HClO$_4$, the solution was evaporated close to dryness. The residue was dissolved with 3 g HNO$_3$ and evaporated close to dryness again. This step was repeated two to three times until the solution appeared clear under 10 times magnifying glass (i.e., complete dissolution). The elemental concentrations were measured with an inductively coupled plasma-mass spectrometer (ICP-MS, VG PlasmaQuad PQ2 Plus). Accuracy determined on artificial solutions and international standard reference rocks was better than 5%. The quantitative detection limit for solutions, set at 10 times the standard deviation on the blanks analyzed during the same run, was, on average, between 10 and 100 parts per trillion (ppt) for the trace elements. Taking into account the dilution factor, the detection limit, in terms of equivalent concentration in the sediment sample, ranged between 25 and 250 ppb (ng g^{-1}).

[11] Baxs is defined as being the total Ba in the sediment minus the Ba associated with the detrital component. This detrital fraction was estimated from measured total Al content and a reference upper crustal Ba/Al ratio of 0.0067 (average value calculated from *Taylor and McLennan* [1985]), assuming that all Al was associated with the detrital fraction and that the reference Ba/Al ratio is representative for the detrital fraction in these sediments. This simplistic approach partitions Ba into a biogenic and a detrital phase, but other Ba components might be relevant [*Dymond et al.*, 1992; *Schroeder et al.*, 1997]. The use of Al as the crustal reference element for oceanic sedimentary material was questioned by *Murray and Leinen* [1996], who showed that a significant component of Al can be scavenged from seawater under regimes of high biogenic particle flux. *Dymond et al.* [1997] furthermore suggested diatoms were the conveyors of this excess Al signal. Because of this, Ti has been put forward as a more appropriate reference element [*Murray and Leinen*, 1996]. Recently, *Yarincik et al.* [2000] pointed out that the excess Al
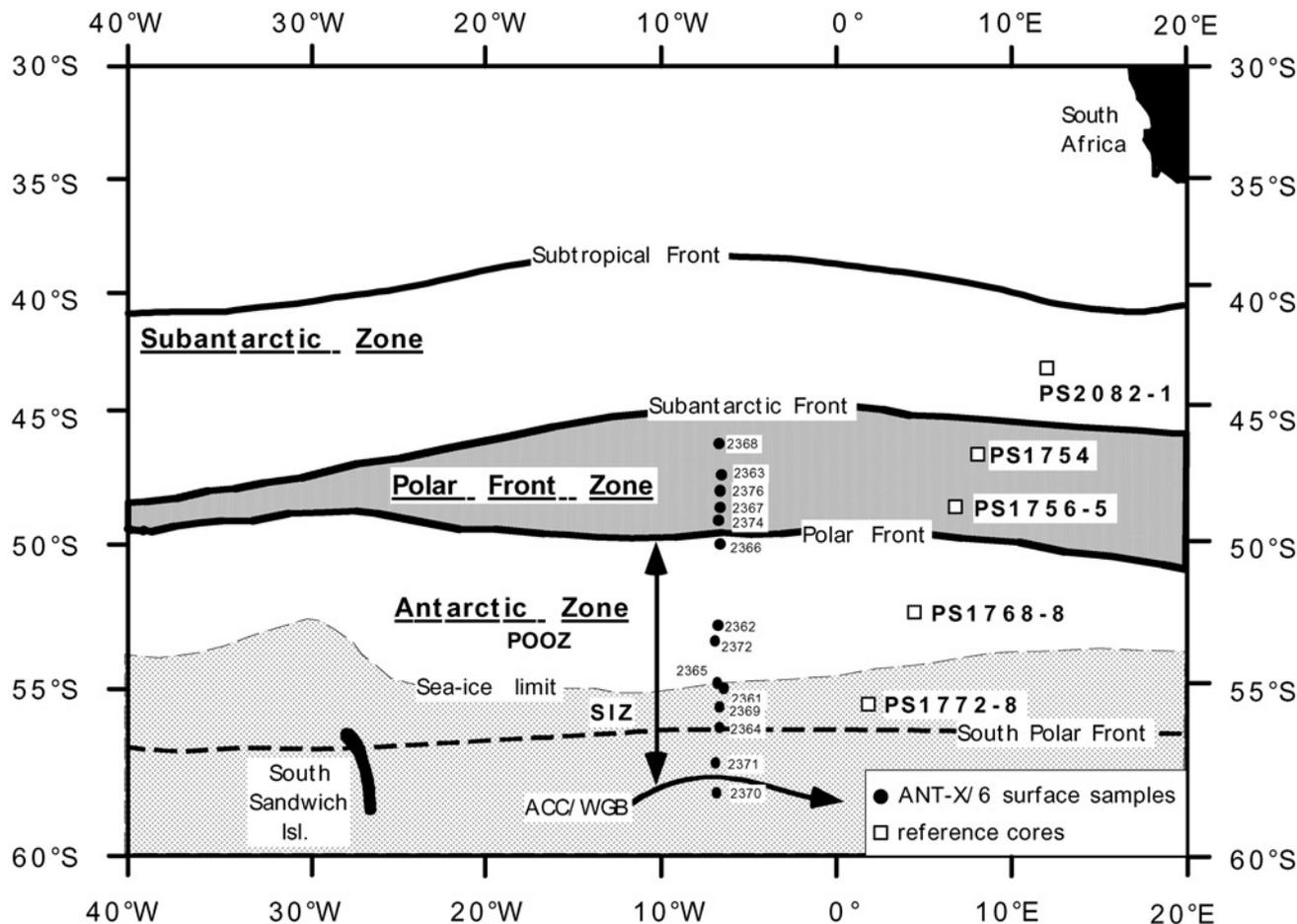
Figure 1a. Map showing the location of the sampled sites (solid circles) and the reference cores (open squares) studied by *Frank et al.* [1996] in the Atlantic sector of the Southern Ocean. The present-day positions of the oceanographic fronts are based on *Peterson and Stramma* [1991] and *Veth et al.* [1997]. The dashed area indicates the northernmost extent of sea ice cover [*Veth et al.*, 1997]. The dark shaded area indicates the position of the Polar Front Zone.

component has to be taken into account only in sediments with <5% terrigenous matter. Consequently, the use of Al for detrital correction remains justified in surface Southern Ocean sediments. However, in situations where the detrital component becomes predominant the choice of the crustal reference ratio has an important impact on the calculated Baxs fraction. A further concern is that reported values of Ba/Al in the lithogenic reference vary significantly, depending on the chosen reference (e.g., Ba/Al$_{ref}$ = 0.004 (wt/wt) [*Gingele and Dahmke*, 1994], Ba/Al$_{ref}$ = 0.0075 [*Nürnberg et al.*, 1997; *Dymond et al.*, 1992], and Ba/Al$_{ref}$ = 0.0092 [*McManus et al.*, 1998]). As a result, the correction for detrital Ba becomes highly unreliable in situations with high contents of lithogenic matter [*Dymond et al.*, 1992; *McManus et al.*, 1998]. The former authors estimate that correction of the detrital fraction is meaningful only for situations with <50% detrital Ba, but the error on this estimation rises to 50% in cases where detrital Ba approaches half of total Ba.

[12] The excess ^{230}Th (^{230}Thxs) content was measured in surface sediments from the Indian sector to quantify the post-depositional sediment redistribution. Samples were prepared by a standard method [*Anderson and Fleer*, 1982]. Approximately 250 mg of dried sediment was spiked with ^{229}Th. Sediments were digested using a triacid attack including HNO$_3$, HClO$_4$, and HF (reagent grade). The solution was evaporated close to dryness twice, and the final residue was redissolved with

concentrated HNO$_3$ then with 2 N HCl. A 100 μL aliquot was then removed for analysis of ^{238}U/^{232}Th. Th was coprecipitated with Fe. After washings, the precipitate was dissolved in 9 N HCl and passed through an ion exchange column (Biorad AG1-X8, 100–200 mesh, preconditioned with 9 N HCl) to remove the Fe. Th was eluted with 9 N HCl. The Th fraction was purified by a second elution on an ion exchange column preconditioned with 8 N HNO$_3$ and then dried to a drop. The Th fraction was diluted with Milli-Q grade water just before analysis by isotope dilution on a Finnigan Mat sector field inductively coupled plasma-mass spectrometer (Element I ICP-MS) at Woods Hole Oceanographic Institution. A complete ICP-MS analysis cycle included 20 s of sampling, 30 s of analysis, and 3 min of rinsing with a 10% HNO$_3$ solution to minimize memory effects. Acid blanks were analyzed prior to each sample, and counts were subtracted from sample counts whenever exceeding 1% of the latter. The drift in the mass discrimination effect was controlled by repeated analysis of a standard solution of known isotopic composition. A tailing correction of the ^{232}Th on mass 230 was performed when necessary.

4.   Results

4.1.   Atlantic Sector of the Southern Ocean

[13] The total barium content in the surface sediments along 6°W ranges between ∼240 and ∼1600 ppm (Table 1). The highest

Figure 1b.   Map showing the location of the sediment sampling sites in the Indian sector of the Southern Ocean. The present-day position of the oceanographic fronts are from *Bareille* [1991] and *Bareille et al.* [1991]. The dashed area limits the oceanic zone covers by ice. The dark shaded area highlights the position of the Polar Front Zone.

values occur in the Antarctic Zone, and the lowest ones coincide with the location of the Polar Front and the Southern Polar Front (Figure 2a). Baxs varies widely, from representing >98% of total Ba in the Antarctic Zone to only 10% close to the sea ice edge. Baxs represents, on average, >80% of total Ba in the Polar Front Zone (88%) and the Antarctic Zone (82%). In the Weddell Gyre Zone, Baxs represents only 50% of the total Ba. The use of Ti or Zr as normative elements does not significantly change the estimates of Baxs, except in two samples where the detrital Ba reaches 50% or more (Table 1; see section 3). The detrital Ba content varies by a factor of 10 across the transect (from 20 to 240 ppm), with its lowest contribution in the POOZ. Zr and Nd display a similar latitudinal profile (Figure 2a).

[14] Baxs is sensitive to changes in sediment composition. No overall correlation is observed between Baxs and $CaCO_3$ (Table 1), but three negative excursions (PS2374, PS2372, and PS2364) of Baxs coincide with carbonate contents >50% (Figure 2b) and suggest a local dilution of Baxs by carbonate phases. To avoid compositional dilution effects, Baxs should be converted into Baxs accumulation rate. The mass accumulation rates were not measured along this transect, but they are known to show large spatial variability in the southern Antarctic Zone (from 5 to 50 cm kyr^{-1} [*Charles et al.*, 1991; *Anderson et al.*, 1998]). Since contents of Ba and Al would be

equally affected by dilution with a third component, variation of the Ba/Al ratio would reflect variation of Baxs that is unaffected by compositional dilution. Therefore it is more appropriate to report the latitudinal distribution of Baxs/Al (wt/wt) ratio (Figure 2b), rather than that of Baxs. The lowest Ba/Al ratio observed at the South Polar Front (0.006, 56°S) is close to the reference post-Archan Australian Shales (PAAS) value [*Taylor and McLennan*, 1985], indicating that nearly all the Ba is lithogenic at this location. The Ba/Al ratio increases by up to a factor of 80 and reaches its highest value (0.47) in the POOZ. The pattern of the Ba/Al profile emphasizes the contrast between the POOZ and the adjacent zones. The POOZ clearly displays Ba/Al ratios up to 10 times higher than those observed for the PFZ and the SIZ.

4.2. Indian Sector of the Southern Ocean

[15] Sampling sites are distributed between the Subantarctic Zone and the Antarctic slope area (Figure 1b). Results are reported by hydrodynamic province and according to latitude within each province (Table 2). The total Ba content varies between ~500 and ~2200 ppm with the highest values measured in the seasonal ice zone (Figure 3a). Note that the lowest Ba values in the POOZ correspond to cores MD84568 and MD84563 from sites with a shallower water column, close to

Table 1. Major and Trace Element Data for Bulk Sediments From Surface Samples of the Atlantic Sector of the Southern Ocean[a]

	Site	Water Depth, m	Latitude, °S	Al$_2$O$_3$, %	TiO$_2$, %	CaO, %	CaCO$_3$ Estimate, %	Total Ba, ppm	Sr, ppm	Zr, ppm	Nd, ppm	Th, ppm	Baxs/Al, %	Baxs/Ti, %	Baxs/Zr, %	Baxs, ppm	Detrital Ba, ppm	Ba/Al, wt/wt
								Geochemical Results					**Ba Partition**					
PFZ	PS2368	3756	46.5	3.0	0.16	32.0	57	935	894	37	7.5	2.1	89	89	88	832	103	0.060
PFZ	PS2363	4040	48.0	4.7	0.26	12.9	23	1026	311	88	8.9	2.7	84	83	73	860	166	0.041
PFZ	PS2376	4091	48.3	2.7	0.15	19.1	34	1365	562	37	7.1	2.0	93	93	92	1272	93	0.097
PFZ	PS2367	3715	49.0	2.6	0.12	18.8	34	1158	572	47	6.0	1.7	92	93	87	1068	90	0.085
PFZ	PS2374	2347	49.6	3.3	0.21	33.8	60	573	309	34	5.2	1.4	80	75	81	458	115	0.033
PFZ Mean				3.2	0.2	23.3	42	1011	530	49	6.9	2.0	88	87	84	898	113	0.063
Antarctic Zone																		
POOZ	PS2366	2060	50.6	0.54	0.03	8.7	16	963	690	10	2.1	0.34	98	98	97	944	19	0.337
POOZ	PS2362	2688	53.0	0.56	0.03	14.9	27	1388	480	14	2.5	0.55	99	98	97	1368	20	0.468
POOZ	PS2372	2341	53.6	2.2	0.14	28.7	51	1079	264	18	3.2	0.65	93	91	95	1004	75	0.095
POOZ	PS2365	3117	55.0	0.89	0.06	4.6	8	1441	428	19	2.0	0.56	98	97	96	1410	31	0.306
SIZ	PS2361	3194	55.0	1.1	0.06	5.4	10	1588	190	20	2.3	0.61	98	97	96	1550	38	0.275
SIZ	PS2369	4059	55.5	9.4	0.51	7.7	14	956	150	76	6.7	1.9	66	65	75	628	328	0.019
SIZ	PS2364	4156	56.0	8.1	0.46	29.5	53	243	297	32	5.7	1.2	12	–	59	28	215	0.006
SIZ	PS2371	3660	57.0	3.1	0.18	2.7	5	1193	113	33	3.1	1.1	91	90	92	1083	110	0.072
Mean				3.2	0.19	12.8	23	1106	326	28	3.4	0.9	82	91	88	1002	104	0.197
WGZ	PS2370	5039	58.3	11.6	0.75	8.2	15	827	152	65	9.0	3.2	51	40	76	421	406	0.013

[a] The estimated carbonate content (CaCO$_3$ Estimate) was based on an estimated stoichiometric amount of CO$_2$ assuming that all the measured CaO is due to carbonate. The barite fraction was defined by the excess Ba fraction. This biogenic Ba fraction is estimated from the bulk sediment composition using Al as a detrital reference with a Ba/Al ratio of 0.0067 [*Taylor and McLennan*, 1985]. The values obtained by applying other normalization elements (Ti and Zr) are also calculated. For comparison with crustal reference the Ba/Al (wt/wt) ratio of each sediment sample is reported. PFZ, Polar Front Zone; POOZ, permanently open ocean zone; SIZ, seasonal ice zone; WGZ, Weddel Gyre Zone.

Table 2. Major and Trace Element Data for Bulk Sediments From Surface Samples of the Indian Sector of the Southern Ocean[a]

										Geochemical Results									Ba Partition				
	Cruise	Site	Water Depth, m	Longitude, °W	Latitude, °S	Al$_2$O$_3$, %	SiO$_2$, %	TiO$_2$, %	CaO, %	CaCO$_3$ Estimate, %	CaCO$_3$ Measured, %	Opal, %	Total Ba, ppm	Sr, ppm	Zr, ppm	Nd, ppm	Th, ppm	Baxs/Al, %	Baxs/Ti, %	Baxs/Zr, %	Baxs, ppm	Detrital Ba, ppm	Ba/Al, wt/wt
SAZ	MD	9406	3315	90.1	44.7	0.93	4.64	0.04	38.7	69			832	1510	11.34^b	5.10	0.57	96	93	92	795	37	0.169
SAZ	MD	94109	3315	90.1	44.7	0.96	5.17	0.05	37.8	68			927	1500	11.83	5.11	0.56	96	97	96	889	38	0.183
SAZ	KR	8801	2920	79.5	46.7	3.09	27	0.34	24.6	44		21	808	816	64.31	9.47	1.90	85	97	96	685	123	0.049
SAZ	KR	8802	3330	82.9	45.8	3.40	27	0.38	24.1	43		23	778	819	68.69	10.1	1.88	83	73	75	643	135	0.043
SAZ	MD	9402	3559	86.5	45.6	2.06	25	0.20	27.1	48		21	1090	1055	37.82	8.04	1.45	93	88	89	1008	82	0.100
SAZ	KR	8806	3850	128.8	49.0	0.76	4.03	0.03	38.9	70		3	644	1400	10.26^b	5.80	0.67	95	88	89	613	30	0.159
SAZ Mean						1.87	15	0.17	32	57			846	1183	34	7.27	1.17	91	86	87	772	74	0.117
PFZ	MD	94104	3460	88.1	46.5	2.57	33	0.25	24.6	44		32	1312	935	48.97	8.62	1.68	92	87	88	1210	102	0.096
PFZ	KR	8803	3420	90.1	46.1	1.65	14	0.11	31.4	56		14	1076	1231	24.39	6.55	0.97	94	93	93	1011	65	0.123
PFZ	MD	88770	3290	96.5	46.0	0.84	7.75	0.04	36.7	66	83	8	778	1280	9.68^c	4.17	0.45^b	96	97	96	744	33	0.176
PFZ	MD	94107	3525	90.2	47.8	2.37	31	0.24	24.6	44		30	1122	826	44.26	7.68	1.52	92	86	88	1028	94	0.089
PFZ	KR	8804	3310	100.1	49.9	1.36	24	0.10	21.7	39		31	1058	722	21.54	4.90	0.95	95	94	94	1004	54	0.147
PFZ	MD	88772	3240	104.9	50.0	1.07	32	0.06	24.9	44	56	31	1440	889	17.92^b	4.39	0.74	97	97	96	1398	43	0.254
PFZ	MD	9404	4036	90.3	50.4	2.62	40	0.26	18.4	33		40	1095	574	51.80	7.89	2.11	90	84	85	990	104	0.079
PFZ	MD	88774	3460	109.9	52.9	0.58	3.91	0.03	38.8	69			755	1421	9.40^c	3.71	0.43^b	97	97	96	732	23	0.245
PFZ	KR	8810	2785.00	144.8	54.2	0.49	48	0.01	13.7	24	22	50	1035	477	11.05^b	2.77	0.32	98	99	97	1015	20	0.396
PFZ Mean						1.51	26	0.12	26.1	47			1075	928	27	5.63	1.02	95	93	93	1015	60	0.178
Antarctic Zone																							
POOZ	MD	84568	2241	72.7	48.6	0.71	74	0.07	2.2	4			505	98	17.44^b	1.96	0.28^b	94	93	90	477	28	0.134
POOZ	MD	84563	1720	68.2	50.7	0.61	52	0.05	6.8	12			504	226	16.44^b	2.29	0.31^b	95	92	94	480	24	0.156
POOZ	MD	88795	1870	68.0	50.8	0.88	67	0.12	8.0	14		72	981	248	19.55^b	2.33	0.28^b	96	97	91	946	35	0.212
POOZ	MD	84562	3550	68.2	51.9	1.03	56	0.06	12.4	22			1313	406	37.50	5.28	0.98	97	97	95	1272	41	0.240
POOZ	KR	8805	3510	109.9	52.9	0.92	53	0.05	8.8	16		56	1186	303	18.22	3.08	0.67	97	99	97	1149	36	0.244
POOZ	KR	8811	2880	144.1	54.9	0.48	48	0.02	17.5	31	19	39	1155	559	11.76^b	2.47	0.21^b	98	92	93	1136	19	0.458
POOZ	MD	84551	2230	73.3	55.0	0.86	63	0.12	8.4	15	11	77	942	262	23^b	2.66	0.36^b	96	10	97	908	34	0.206
POOZ	KR	8812	3020	145.3	56.4	0.40	48	0.01	17.5	31		70	1062	509	10^b	1.60	0.16^b	99	92	91	1046	16	0.506
POOZ	MD	84550	4080	71.4	56.8	1.09	73	0.14	4.9	9			1146	183	32	3.66	0.61	96	99	97	1103	43	0.199
POOZ	KR	8813	3740	144.6	57.9	0.46	58	0.01	9.4	17		48	1439	300	16^b	2.24	0.38^b	99	90	89	1421	18	0.591
SIZ	MD	85540	3960	86.4	60.7	4.55	72	0.28	1.9	3			1822	130	67	13	6.61	90	92	86	1641	181	0.076
SIZ	KR	8830	4300	93.2	61.0	6.17	66	0.35	0.6	1	0	49	1855	116	127	15	7.25	87	86	85	1610	245	0.057
SIZ	KR	8814	4200	144.4	61.3	3.58	63	0.20	4.4	8	7	55	1559	186	73	7.48	4.01	91	74	69	1417	142	0.082
SIZ	KR	8829	3790	95.9	62.5	9.05	49	0.47	0.9	2		30	2164	138	102	23	12	83	74	75	1805	359	0.045
SIZ	KR	8815	3880	141.9	63.3	8.83	60	0.52	1.7	3	0	27	1328	160	135	20	9	74	77	57	977	351	0.028
SIZ	KR	8823	3292	117.3	63.3	11.20	42	0.59	5.4	10		21	1523	261	122	29	14	71	74	59	1079	444	0.026
SIZ	KR	8827	1240	101.2	63.7	8.05	51	0.59	2.8	5			1701	207	235	32	15	81	58	40	1382	320	0.040
SIZ	KR	8824	2600	116.4	63.8	10.87	55	0.57	3.4	6	0	18	1475	230	196	30	14	71	–	–	1044	432	0.026
SIZ	KR	8822	3150	119.5	64.7	12.65	62	0.67	1.9	3		20	1043	198	203	39	18	52	–	–	541	502	0.016
Mean						4.3	59	0.26	6.3	11			1300	249	77	12	5.5	88	87	83	1128	172	0.176

[a] The estimated carbonate content (CaCO$_3$ Estimate) was based on an estimated stoichiometric amount of CO$_2$ assuming that all the measured CaO is due to carbonate. Such assumption leads in general to an overestimation of the real carbonate content. The estimation is controlled by direct measurements of the carbonate content (CaCO$_3$ Measured) based on ignition loss on a few samples (data from *Bareille* [1991] and *Bareille et al.* [1991]). SAZ, Subantarctic Zone; PFZ, Polar Front Zone; POOZ, permanently open ocean zone; SIZ, seasonal ice zone.

[b] Values correspond to semiquantitative data (i.e., value between 1 and 3 times the detection limit).
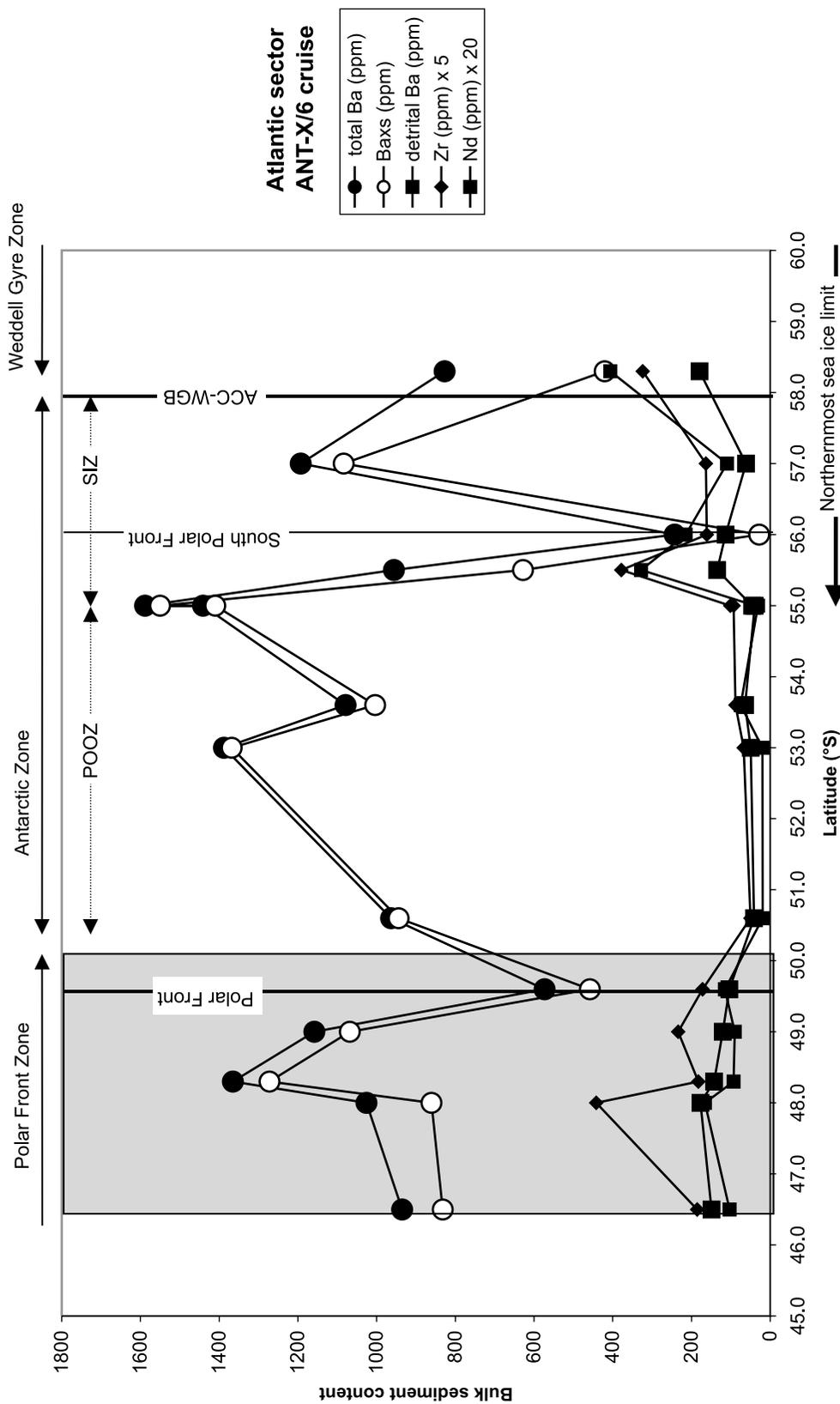
Figure 2a. Ba (total, excess, or detrital fraction), Zr, and Nd content in surface sediments along a north-south transect at 6°W in the Atlantic sector of the Southern Ocean (ANT X/6 expedition). The shaded area indicates the position of the Polar Front Zone. Data are from Table 1.
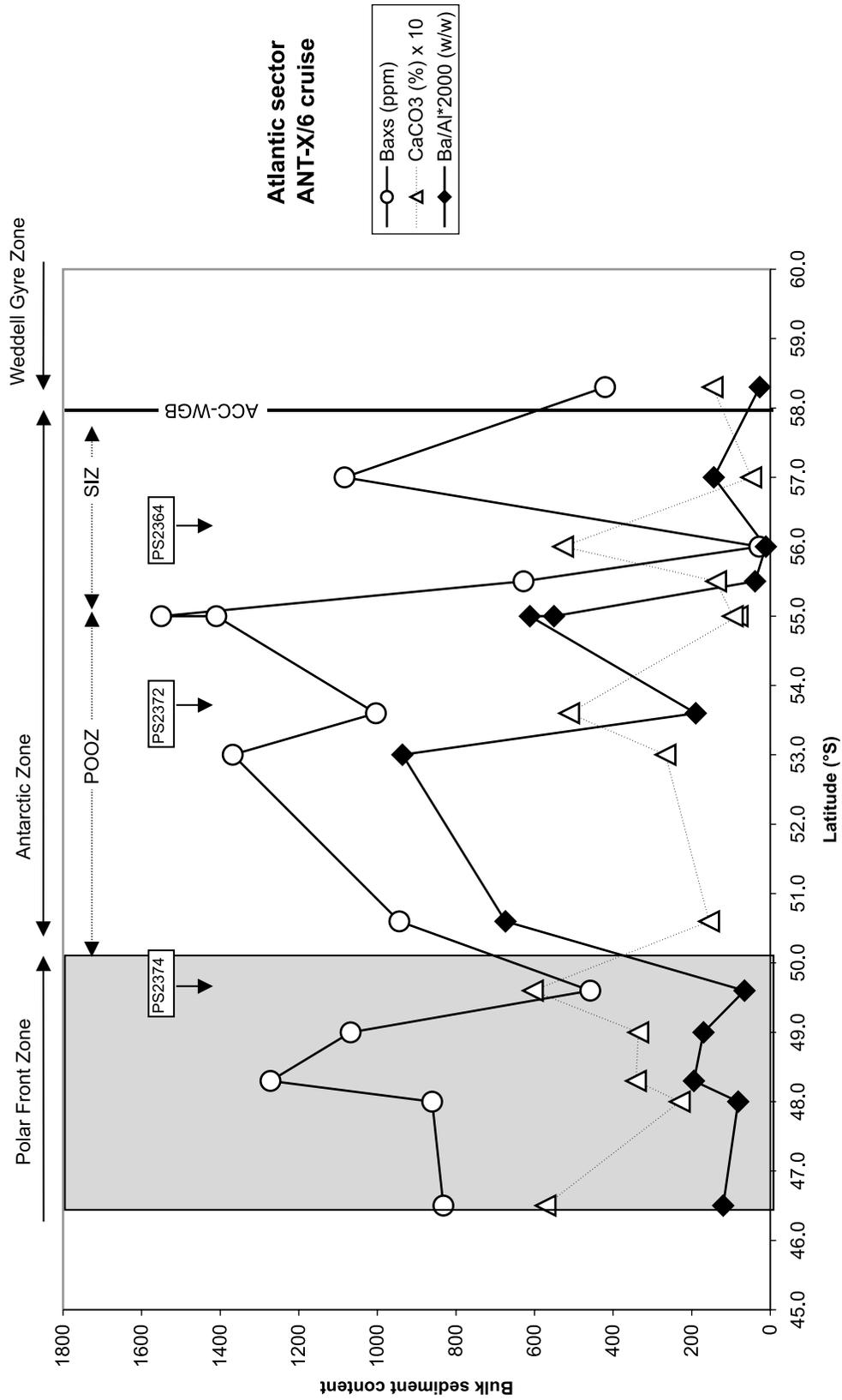
Figure 2b. Excess Ba, carbonate content, and Ba/Al (wt/wt) ratio in surface sediments from the north-south transect at 6°W across the Atlantic sector of the Southern Ocean (ANT X/6 expedition). The comparison of Baxs pattern and Ba/Al ratio help to identify any dilution of Baxs due to a change of sedimentary composition. Note that there is no systematic dilution of Baxs content by carbonates, except in three carbonate-rich samples (PS2374, PS2372, and PS2364).
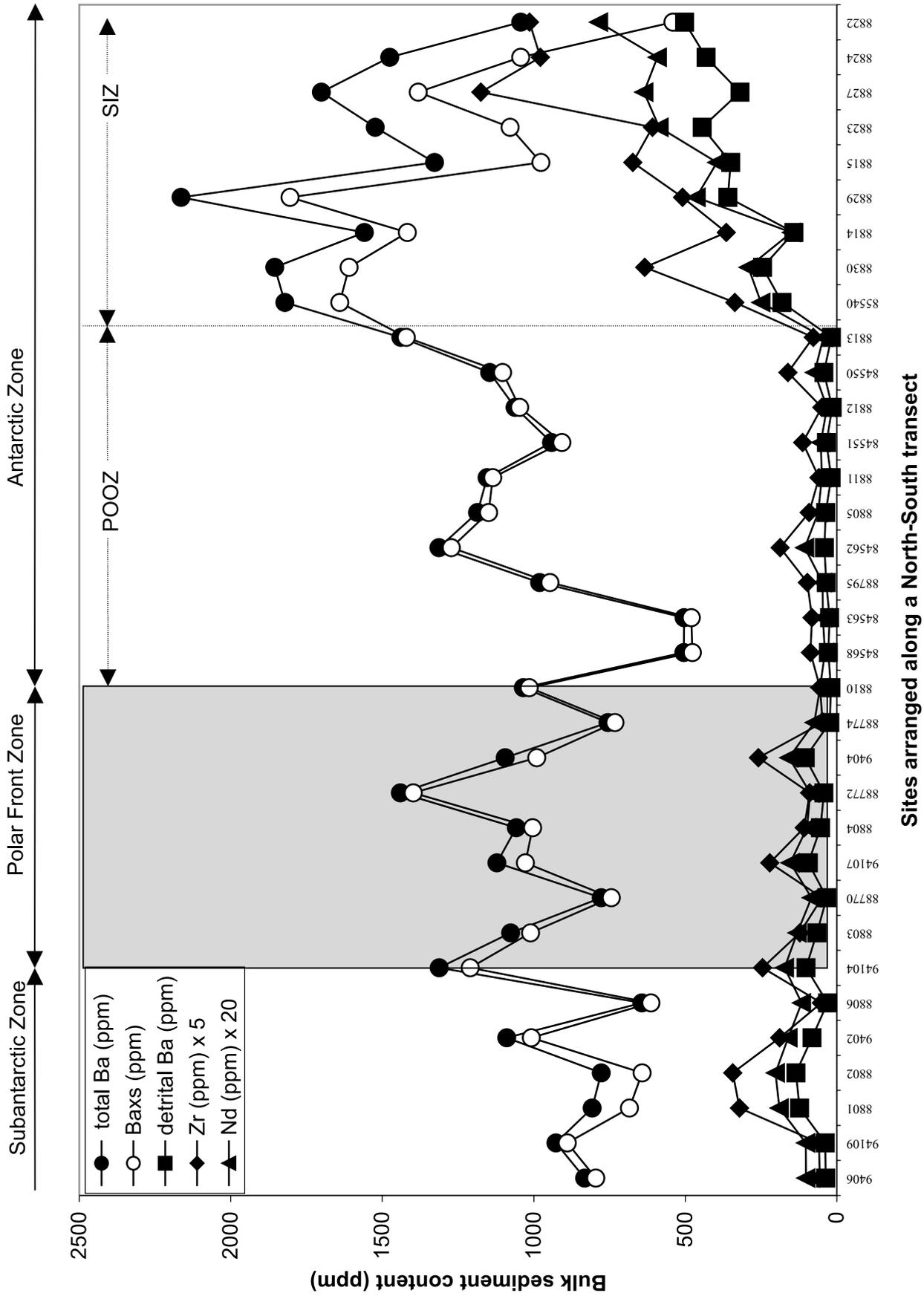
Figure 3a. Ba (total, excess, or detrital fraction), Zr, and Nd content in surface sediments collected across the Indian sector of the Southern Ocean. The shaded area corresponds to the Polar Front Zone.
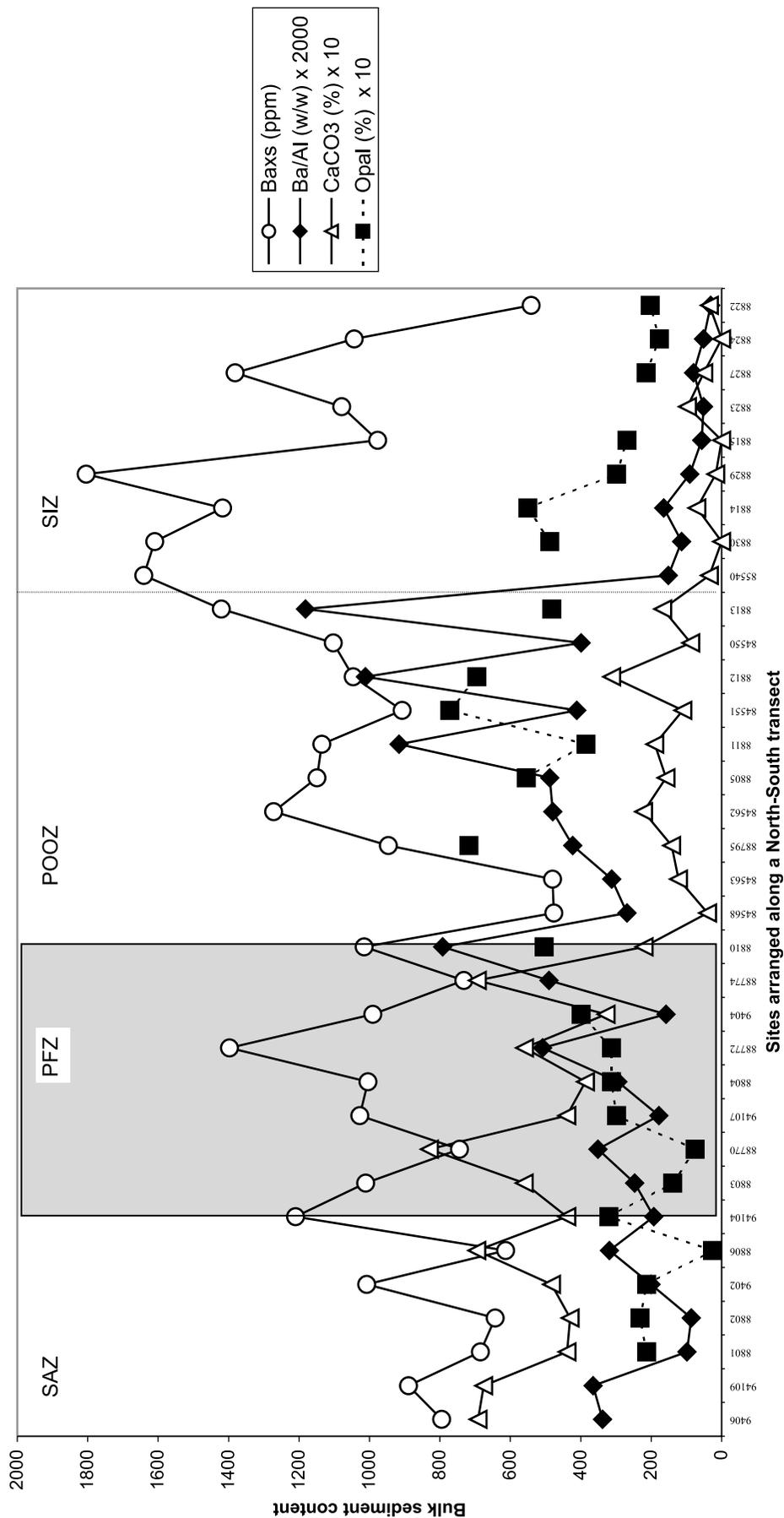
Figure 3b. Excess barium, carbonate content, opal content, and Ba/Al (wt/wt) ratio in surface sediments from the Indian sector of the Southern Ocean. The shaded area corresponds to the Polar Front Zone. Note the absence of an obvious relationship between carbonate or opal content and Baxs. However, the high mean carbonate content in the northern part of the transect coincides with the lowest mean Baxs content. The Ba/Al ratio pattern is different from the Baxs pattern, emphasizing some compositional dilution of Baxs.
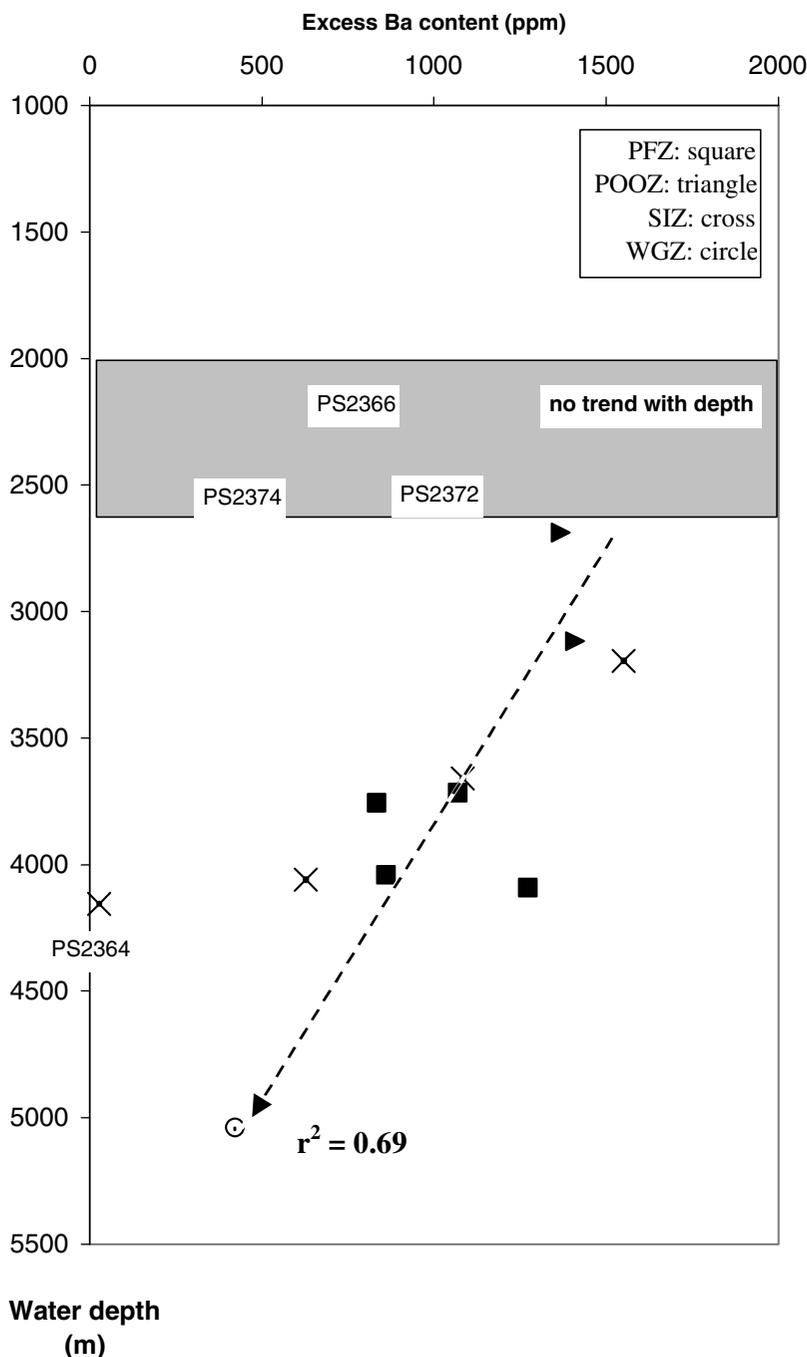
Figure 4a. Excess Ba content reported as a function of the water column depth for the Atlantic sector of the Southern Ocean. Data are from Table 2. For the samples deeper than 2500 m water depth the Baxs content decreases with increasing water depth. This may reflect a higher dissolution of barite crystals in progressively undersaturated waters.

Kerguelen Island. As observed for the Atlantic sector, most of the Ba is Baxs (52–99%; Table 2). The detrital Ba content is low from the Subantarctic Zone to SIZ. It then increases significantly through the SIZ to reach 140–500 ppm in the vicinity of the Antarctic slope. Zr, Nd, and Th also display a significant increase south of 60°S. The lowest fractions of Baxs (down to 40%) are observed south of 60°S in the SIZ and coincide with the highest contents of detrital Ba (142–502 ppm; Table 2). Highest carbonate

contents occur north of the Polar Front. Carbonate contents decrease southward to values as low as 1% in the SIZ (Figure 3b). The Baxs pattern cannot result from dilution with carbonates since Baxs and carbonates are not correlated ($r^2 = 0.20$; Table 2). For the Indian sector sediments the Baxs accumulation rates could be estimated for each sample using the mass accumulation rate deduced from the local linear sedimentation rate and the measured dry bulk density [*Bareille*, 1991; *Bareille et al.*, 1991, 1998]. However, accumulation

rates may be affected by sediment reworking (focusing and winnowing). These impacts will be discussed in section 5.2.

[16] The Ba/Al ratios range from 0.016 to 0.591, with highest values recorded in the POOZ, also characterized by the highest opal content (Figure 3b and Table 2). The pattern of the Ba/Al ratio does not follow the latitudinal trend of the Baxs, emphasizing a compositional dilution effect on the Baxs in the Indian sector of the Southern Ocean.

5. Discussion

[17] Unlike margin environments where redox conditions and/or advection of detrital materials may limit the use of sedimentary Baxs as a proxy of export production [e.g., *Brumsack*, 1989; *Von Breymann et al.*, 1992; *Dymond et al.*, 1992; *McManus et al.*, 1994], Baxs appears to be a promising tracer of export production in open ocean systems [e.g., *Nürnberg et al.*, 1997; *Gingele and Dahmke*, 1994]. It was suggested by *François et al.* [1995] that the higher dissolved Ba contents in intermediate and deep waters probably do not affect the water column Baxs flux, as originally suggested by *Dymond et al.* [1992]. We will consider therefore only the François et al. and Nürnberg et al. approaches. Export production P may be estimated as a function of the water column Baxs flux (FBaxs in g cm^{-2} yr^{-1}) and water depth Z (in m) ((1), from *Nürnberg et al.* [1997]) or only as a function of the Baxs flux with no dependence on depth ((2), from *François et al.* [1995]):

$$E\,P\big(\text{g cm}^{-2}\ \text{yr}^{-1}\big) = 3.56(\text{FBaxs})1.504\,Z^{-0.0937} \qquad (1)$$

$$E\,P\big(\text{g cm}^{-2}\ \text{yr}^{-1}\big) = 1.95\,(\text{FBaxs})^{1.41}, \qquad (2)$$

where E is export.

[18] Both equations are conceptually related [see *François et al.*, 1995; *Nürnberg*, 1995] and give similar results. Equation (2) is a simplification of (1) and implies annual average Baxs fluxes remain constant with depth. This approach assumes that there is no advective supply of Baxs. Widespread occurrence of reducing conditions in margin environments would dissolve barite [*François et al.*, 1995; *Von Breymann et al.*, 1992], and as a consequence, possible horizontal advective fluxes would be devoid of barite. This assumption, however, has recently been invalidated. In a study on Ba fluxes in a NE Atlantic Margin environment, *Fagel et al.* [1999] observed enhanced Baxs fluxes outside the bloom period which were related with lateral advection transport carrying Baxs and lithogenic particles to the sampling site. This observation, although of local importance, underlines the necessity to compute export production from a reasonably large time series to prevent (or at least reduce) sporadic effects.

[19] In the present work, export production was estimated using (1) originally deduced from open ocean sediment trap data. For sediments, however, the actual accumulation rate may be different from the vertical flux. Two processes have to be corrected for in order to estimate the true vertical Baxs flux. First, the preserved Baxs accumulation rate might differ from the Baxs rain rate because of partial dissolution of barite at the seawater-sediment interface prior to burial. Second, the Baxs accumulation rate may be affected by sediment reworking as a result of bottom currents.

5.1. Dissolution of Barite at the Water Column-Sediment Interface

5.1.1. Estimation of the water column Baxs preservation rate. [20] Application of (1) to the sedimentary environment requires that the preservation rate during exposure of the Baxs phase at the water column-sediment interface before burial is known. *Dymond et al.* [1992] proposed the following algorithm relating the Baxs preservation rate as a function of the sediment mass accumulation rate (AR) (in μg cm^{-2} yr^{-1}):

$$\text{FBaxs} = \text{AR Baxs measured}/\text{DP}(\%), \qquad (3)$$

where DP is degree of preservation and

$$\text{DP}(\%) = 20.9 \log (\text{MAR}) - 20.3, \qquad (4)$$

where MAR is mass accumulation rate. The Dymond et al. algorithm has been applied in many paleoproductivity reconstructions based on sedimentary Baxs [*Gingele et al.*, 1999]. Its predictive capacity has been invalidated in only in a few studies, showing that preservation efficiencies could be related to diagenetic remobilization of Ba [*Paytan et al.*, 1996; *McManus et al.*, 1999]. For instance, recent studies [*McManus et al.*, 1999] suggest diagenetic dissolution of barite crystals even in suboxic conditions, such as would be favored in areas of high mass accumulation. The application of (3) implies that bottom waters are undersaturated with respect to barite. In section 5.1.2, we show that a correction for dissolution through application of (4) is probably justified for most of the oceanic basins, except in shallow bottom waters south of the Polar Front.

5.1.2. Influence of the barite saturation index of bottom waters. [21] For the Atlantic sector of the Southern Ocean we observed that sedimentary Baxs content decreased with increasing water depth for sites deeper than 2500 m (Figure 4a). The negative linear correlation coefficient is 0.69, if sample PS2364 is excluded. We suspect incorrect calculation of Baxs content for this sample because of a high content of the detrital phase (see section 3). While the variability in the Baxs transect (Figure 2b) is probably in part due to latitudinal variability in surface productivity and water column Baxs flux, it is probable that variable barite dissolution is also a contributing factor. In the Antarctic Zone of the Southern Ocean the barite saturation index (SI) isopleth of 0.90 (i.e., the threshold between saturation and undersaturation) stays, in general, close to the 2000 m isobath [*Monnin et al.*, 1999]. In the vicinity of the Polar Front the regular pattern of the SI isolines is affected by abrupt seabed bathymetry changes. North of the Polar Front the whole water column is undersaturated with a barite saturation index <0.7. For the ANT X/6 transect it was noticed that the barite saturation index is negatively correlated ($r^2 = 0.95$; Figure 4b) with hydrostatic pressure (or water column height) whatever the hydrodynamic zone (C. Monnin, unpublished results, 2000). This regression was used to calculate the barite saturation index for all surface sediment sampling sites (Table 3). For SI < 0.89, Baxs in surface sediments decreases with decreasing barite saturation index ($r^2 = 0.69$; Figure 4b), reflecting the effect of hydrostatic pressure. This suggests that dissolution of settled barite would be greater for a deeper seafloor. In the Indian sector, barite SI values are not available for the same location from where surface samples were taken, but they are for a north-south transect at 30°E (CIVA-1 section (C. Monnin, unpublished results)). These data show that the upper 1500–2000 m of the water column is saturated with respect to barite with SI values ranging between 0.9 and 1.1, as observed for the 6°W transect. Thermodynamic calculations thus suggest that south of the Polar Front, barite should not dissolve at the sediment-water interface for a water column shallower than 2500 m.

5.1.3. Preservation rate. [22] In the Atlantic sector, two sites in the POOZ underlie a relatively shallow water column (<2500 m) and are characterized by a high barite SI (≥~0.90; Table 3). At these sites, settled barite could thus be totally preserved, provided conditions of oxicity and saturation within the sediment favor barite integrity. In the Indian sector, two

Excess Ba content (ppm)
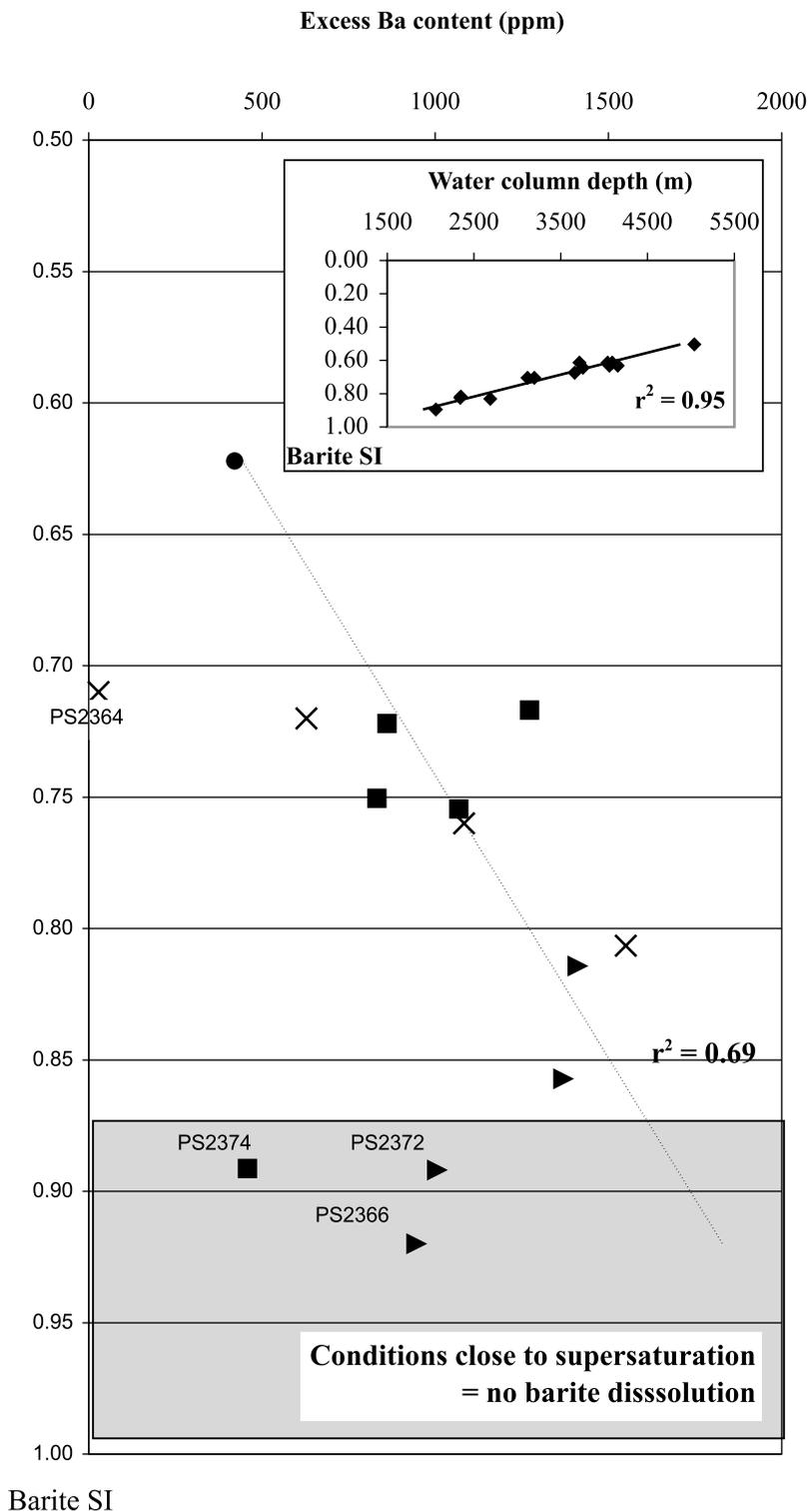
Barite SI

Figure 4b. Excess Ba content reported as a function of the local barite saturation index (SI). Barite saturation index was calculated from the regression line with water column depth shown in the insert. The thermodynamic calculation of the barite saturation index is based on ANT X/6 data (C. Monnin, unpublished results). Barite should not dissolve in waters having a barite SI $\geq$ ~0.90 (shaded area). See text for explanation.

samples from shallower areas in the POOZ may also be unaffected by barite dissolution (Table 4).

[23] For all the other (deeper) sites the preservation rates are estimated using (4). In the Indian sector the preservation rates vary between 35 and 61%, using measured mass accumulation rates (Table 4). The SIZ is characterized by the lowest preservation rates. *Frank* [1996] reported similar preservation rates, ranging from ~40 to 60% for a NNE-SSW 4°–12°E transect

Table 3. Export Production Estimates for the Surface Sediments in the Atlantic Sector of the Southern Ocean Using ANT X/6 Data[a]

Sample	Environment	Latitude, °S	Water Depth, m	Baxs, ppm	SI	^{230}Thxs,[b] dpm/g	Focusing Factor	Focusing, %	Preserved VR Baxs, Mg cm^{-2} kyr^{-1}	Preservation Rate,[c] %	VRR Baxs, mg cm^{-2} kyr^{-1}	Export Production, g C m^{-2} yr^{-1}
PS2368	PFZ	46.50	3756	832	0.75	10.05	10	90	0.82	45	1.82	4.0
PS2363	PFZ	48.00	4040	860	0.72	10.31	10	90	0.89	45	1.97	4.5
PS2376	PFZ	48.30	4091	1272	0.72	13.83	14	93	0.99	45	2.20	5.3
PS2367	PFZ	49.00	3712	1068	0.75	10.00	10	90	1.04	45	2.32	5.8
Mean PFZ				1008		11.05	11	91	0.93	45	2.08	4.9
PS2366	POOZ	50.60	2060	944	0.92[d]	3.66	4	73	1.40	60(100)[d]	2.33(1.40)[d]	6.2(2.9)[d]
PS2362	POOZ	53.00	2688	1368	0.86	4.93	5	80	1.96	60	3.27	10
PS2372	POOZ	53.60	2341	1004	0.89[d]	6.00	6	83	1.03	60(100)[d]	1.72(1.03)[d]	3.9(1.8)[d]
PS2365	POOZ	55.00	3117	1410	0.81	4.94	5	80	2.34	60	3.90	13
Mean POOZ				1182		4.88	5	80	1.68	60(100)	2.8(2.4)	6.9(8.3)
PS2361	SIZ	55.10	3194	1550	0.81	5.57	6	82	2.34	39	5.99	25
PS2369	SIZ	55.50	4059	628	0.72	7.66	8	87	0.88	39	2.24	5.5
PS2364[e]	SIZ	56.00	4156	28[e]	0.71	7.81	8	87	0.04[e]	39	0.10[e]	0.05[e]
PS2371	SIZ	57.00	3660	1083	0.76	7.61	8	87	1.37	39	3.51	11
Mean SIZ				1087		7.16	7	86	1.53	39	3.92	13.7
PS2370	WGZ	58.30	5039	421	0.62	11.63	12	91	0.47	39	1.21	2.15

[a] Sample PS2364 has not been taken into account to calculate the mean export production value. The barite saturation index has been calculated for each sample depth according to the regression line between SI and water depth shown in Figure 4b.

[b] Data are from *Walter et al.* [1997].

[c] Estimation is from *Frank et al.* [1996].

[d] For two samples in the POOZ, two estimates of export production are reported: the first value took into account the *Dymond et al.* [1992] algorithm for calculation of the preservation rate, and the second value (in parentheses) assumed a 100% preservation rate. See text for explanation.

[e] Sample is not taken into account in the mean.

Table 4. Export Production Estimates for the Surface Sediments in the Indian Sector of the Southern Ocean Using APSARA DATA[a]

Sample	Environment	Water Depth, m	Baxs, ppm	Dry Bulk Density, g cm^{-3}	LSR, cm kyr^{-1}	MAR, mg cm^{-2} yr^{-1}	^{230}Thxs, dpm g^{-1}	Focusing Factor	Focusing, %	Preserved VRR Baxs, mg cm^{-2} kyr^{-1}	Preservation Rate, %	VRR Baxs, mg cm^{-2} kyr^{-1}	Export Production, g C m^{-2} yr^{-1}
MD 9406	SAZ	3315	799	0.95	4.2	4.0	7.28	3.3	71	0.96	54	1.77	3.9
MD 94109	SAZ	3315	893	0.95	4.2	4.0	7.28	3.3	71	1.07	54	1.98	4.7
KR 8801	SAZ	2925	698	0.58	4.5	2.6	5.19	1.8	45	1.03	50	2.07	5.0
KR 8802	SAZ	3480	657	0.51	10	5.1	9.17	5.1	81	0.66	56	1.17	2.1
MD 9402	SAZ	3572	1017	0.66	13.3	8.8	9.93	9.3	90	0.96	61	1.57	3.3
Mean SAZ					7.2	4.9	7.77	4.6	72	0.94	55	1.7	3.8
MD 94104	PFZ	3460	1221	0.62	11.7	7.2	NM[b]	10.0	90[b]	0.88	59	1.49	3.0
KR 8803	PFZ	3400	1018	0.72	5.2	3.7	NM[b]	3.3	70[b]	1.14	53	2.13	5.2
MD 88770	PFZ	3290	748	0.68	6.8	4.6	NM[b]	3.3	70[b]	1.04	55	1.88	4.3
MD 94107	PFZ	3525	1038	0.69	8.3	5.7	9.85	6.1	84	0.98	57	1.71	3.7
KR 8804	PFZ	3350	1010	0.46	6.9	3.2	3.17	1.2	17	2.80	52	5.40	21
MD 88772	PFZ	3240	1402	0.46	5.8	2.7	7.99	2.5	62	1.50	50	2.97	8.6
MD 9404	PFZ	4036	1002	0.51	4.6	2.3	11.9	2.6	63	0.89	49	1.82	4.0
MD 88774	PFZ	3330	735	0.26	25	6.4	6.86	5.0	81	0.94	58	1.61	3.4
Mean PFZ					10.1	4.1	7.95	3.5	61	1.42	54	2.4	6.7
MD 88795	POOZ	1950[c]	950	0.32	5.8	1.9	24.9	9.2	90	0.20	47(100)[c]	0.41(0.20)[c]	0.47(0.15)[c]
KR 8805	POOZ	3510	1153			2.6[d]	NM[b]	10	90[b]	0.30	50	0.60	0.77
MD 84551	POOZ	2230[c]	911	0.29	11.5	3.3	NM[b]	2.5	60[b]	1.22	52(100)[c]	2.33(1.22)[c]	6.2(2.3)[c]
Mean POOZ					13.1	3.9	13.2	6.0	76	0.81	47(100)	1.1(0.67)	2.5(1.1)
KR 8815	SIZ	3880	1014	0.53	2.2	1.2	6.82	0.8	−19	1.52	43	3.55	11
KR 8822	SIZ	3140	594	0.53	3.2	1.7	1.65	0.3	−182	2.97	46	6.42	27
Mean SIZ					6.2	2.3	7.24	2.4	−42	1.77	45	5.0	19

[a] Dry bulk density and linear sedimentation rates are from *Bareille* [1991] and *Bareille et al.* [1991]. NM, not measured.

[b] Data provided by L. Dezileau [see *Dezileau et al.*, 2000].

[c] For two samples in the POOZ, two estimates of export production are reported: the first value took into account the *Dymond et al.* [1992] algorithm for calculation of the preservation rate, and the second value (in parentheses) assumed a 100% preservation rate.

[d] The mass accumulation rate was not determined for sample KR8805. We use for calculation the value of 2.6 mg cm^{-2} yr^{-1}, i.e., the mean MAR value of the two samples recovered in the POOZ area.

Table 5. Comparison of Export Production Estimates for the Atlantic and the Indian Sectors of the Southern Ocean

Material	Proxy	Export Production, g C m⁻² yr⁻¹	Environment				Reference
			SAZ	PFZ	POOZ	SIZ	
Atlantic Sector							
ANT X/6	surface sediment	Baxs	–	4.0–5.8	1.8–13	5.5–25	this work
ANT X/6	surface sediment	Baxs	–	4.9	3.8	14	*Dehairs et al.* [1991]
ANT X/6	particulate Ba	consumption O_2	–	2.73	1.74	1.09	*Rutgers van der Loeff et al.* [1997]
ANT X/6	particulate matter	^{234}Th	–2 bloom⁻¹	9.6	3.6	–	*Nürnberg* [1995]
PF3	traps	Baxs	–	5.6	1.3	–	*Nürnberg* [1995]
PF3	traps	Baxs	–2 bloom⁻¹	9.9–10.2	1.3	–	modified from *Nürnberg* [1995]
ANT X/6	model	SWAMCO model	–	7.6	1.2	–	*Lancelot et al.* [2000]
12°–4° transect	Holocene sediment	Baxs	2.6	7–10	14	4.5	*Frank* [1996], *Frank et al.* [1996]
Atlantic sector	Holocene sediment	Baxs	3–4	5–10	15–24	5	*François et al.* [1997]
Indian Sector							
APSARA cores	Holocene sediment	Baxs	2.1–5.0	3.0–21	0.15–6.16	11–27	this work
APSARA cores	Holocene sediment	Baxs	3.8	6.7	1.1–2.5	19	this work
Indian sector	Holocene sediment	Baxs	–	–	22	–	*François et al.* [1997]

in the Atlantic sector (PFZ, 41–45% for MAR = 1–1.56 mg cm⁻² yr⁻¹; POOZ, 56–60% for MAR = 5–8 mg cm⁻² yr⁻¹; SIZ, 37–39% for MAR = 0.65–0.73 mg cm⁻² yr⁻¹). We will assume that the preservation rates obtained for the nearby NNE-SSW transect studied by Frank et al. apply for the ANT X/6 transect studied here.

[24] We compare the Baxs flux of a sediment trap deployed in the vicinity of the Polar Front in the Atlantic sector (PF3; 50.7°S, 5.5°E; traps at 600 and 3200 m [*Nürnberg*, 1995]) with the Baxs flux of the closest surface sediment (PS1756-5, water depth of 3787 m [*Frank*, 1996]) (Figures 1a and 1b). The trapping efficiencies based on annual ^{230}Th fluxes were estimated at 67 and 47% for the 600 and the 3200 m traps, respectively [*Walter*, 1998]. The sedimentary Baxs flux (2.1 mg cm⁻² kyr⁻¹) represents 64% of the Baxs flux in the 3200 m trap (3.3 mg cm⁻² kyr⁻¹) and 92% of the flux in the 600 m trap (2.3 mg cm⁻² kyr⁻¹).

5.2. Influence of Sediment Focusing

[25] It has been suggested that the highest mass accumulation rates result from lateral advection of sediment induced by strong abyssal currents, a common situation in the Southern Ocean [*François et al.*, 1993; *Kumar*, 1994; *Frank et al.*, 1996]. In the vicinity of the ANT X/6 transect, *Frank et al.* [1996] observed large discrepancies between MAR and VRR estimated from ^{230}Th and ^{231}Pa fluxes. They interpreted this discrepancy as evidence of sediment focusing. The effect of postdepositional sediment redistribution on Baxs accumulation can be corrected for by normalizing Baxs fluxes to excess ^{230}Th activity in sediments as follows [*François et al.*, 1993]:

$$\text{PBaxsRR}\left(\text{mg cm}^{-2}\,\text{kyr}^{-1}\right) = \left(\rho\, z\, [\text{Baxs}]\right) \big/ \left[^{230}\text{Thxs}\right], \qquad (5)$$

where PBaxsRR is preserved Baxs rain rate, ρ is production of ^{230}Th in the water column, equal to 2.63 disintegration per minute (dpm) cm⁻² kyr⁻¹ for a 1000 m water column, Z is water column height (in km), [Baxs] is measured Baxs content in the surface sediment (in ppm), and [^{230}Thxs] is measured activity in the surface sediment (in dpm g⁻¹). This method is based on the assumption of a constant flux of ^{230}Th to the sediment in balance with the rate of ^{230}Th production in the overlying water column. It does not take into account possible ^{230}Th removal due to lateral transport (i.e., boundary scavenging). *François et al.* [1997] estimated the accuracy of the reconstructed fluxes at 40% owing to this boundary scavenging effect.

5.2.1. Atlantic sector. [26] Excess ^{230}Th activity has been measured for the ANT X/6 surface samples [*Walter et al.*, 1997] (Table 3). The highest excess ^{230}Th activity values are reported for the PFZ (mean of 11.05 dpm g⁻¹) and the Weddell Gyre Zone (11.63 dpm g⁻¹). The POOZ is characterized by the lowest excess ^{230}Th activities (mean of 4.88 dpm g⁻¹), but these are highly variable. Such excess ^{230}Th activities indicate that 73–93% of the mass accumulation rate is accounted for by sediment focusing (4 < focusing factor <14). *Frank* [1996] reported a similar impact of sediment reworking along their nearby NNE-SSW 4°–12°E transect (Figure 1a; focusing effect on MAR ranges from 76 to 96% in the SAZ).

[27] For the ANT X/6 transect the preserved rain rate of Baxs obtained from (5) varies by a factor of 5, from a minimum of 0.5 mg cm⁻² kyr⁻¹ in the Weddell Gyre Zone up to 2.3 mg cm⁻² kyr⁻¹ in the Antarctic Zone (Table 3). The POOZ is characterized by the highest mean value of preserved vertical Baxs flux (1.7 mg cm⁻² kyr⁻¹), a value slightly higher than the mean SIZ value (1.5 mg cm⁻² kyr⁻¹) but nearly twice as large (1.8) as the PFZ value (0.9 mg cm⁻² kyr⁻¹). For the nearby NNE-SSW transect studied by *Frank* [1996], estimates of preserved Baxs fluxes are systematically higher than our esti-

mates (1.5 mg cm^{-2} kyr^{-1} for PFZ, 2.50 mg cm^{-2} kyr^{-1} for POOZ, and 0.7 mg cm^{-2} kyr^{-1} for SIZ), but the Baxs flux ratio between POOZ and PFZ is similar (1.7 mg cm^{-2} kyr^{-1}). Because of their proximity we expect the accuracy of the ^{230}Th corrections to be similar for the two transects.

5.2.2. Indian sector. [28] The spatial heterogeneity of the mass accumulation rates (from 0.5 to 8.8 mg cm^{-2} yr^{-1}; Table 4) reflects sediment reworking processes. For the APSARA sediments we estimated the magnitude of the sediment redistribution via ^{230}Thxs correction (Table 4). The reported ^{230}Thxs activity does not take into account any age correction. The ^{230}Thxs activity displays a larger range of variation (1.65–24.9 dpm g^{-1}) than observed for the Atlantic sector, reflecting partly the wide geographical distribution of the samples. Lateral advection accounts for 17–90% of the measured MAR (1.2 < focusing factor < 10). For the POOZ our estimate of sediment focusing impact on MAR (60–90%) is in agreement with values (70–90%) reported by *François et al.* [1997] for the same general area. It appears that the highest measured accumulation rates in cores MD9402 and MD94104 (7.2–8.8 mg cm^{-2} yr^{-1}) are primarily due to sediment focusing. By contrast, in the SIZ, the low mass accumulation rates (<1.7 mg cm^{-2} yr^{-1}) and a focusing factor <1 reflect sediment winnowing.

[29] After correction for sediment redistribution, the preserved rain rates of Baxs (Table 4) vary by a factor of 2–6 within the same oceanic zone (SAZ, 0.7–1.1 mg cm^{-2} kyr^{-1}; PFZ, 0.9–2.8 mg cm^{-2} kyr^{-1}; POOZ, 0.2–1.2 mg cm^{-2} kyr^{-1}; SIZ, 1.5–3.0 mg cm^{-2} kyr^{-1}). Note that with the exception of the POOZ, the mean preserved rain rate of Baxs (mean PFZ is 1.4 mg cm^{-2} kyr^{-1} but is 1.1 mg cm^{-2} kyr^{-1} if one sample is excluded; mean SIZ is 1.8 mg cm^{-2} yr^{-1}) is in the range but is 10% higher for the Atlantic sector (PFZ, 0.9 mg cm^{-2} kyr^{-1}; SIZ, 1.6 mg cm^{-2} kyr^{-1}; Table 3). The mean preserved rain rate of Baxs in the Subantarctic Zone is at least 10% lower than the mean measured in the PFZ. By contrast, the POOZ is characterized by the lowest preserved Baxs rain rates in this sector, with a mean value (0.8 mg cm^{-2} kyr^{-1}) 2 times lower than the mean reported for the Atlantic sector (1.7 mg cm^{-2} kyr^{-1}).

5.3. Export Production Estimate

[30] Preserved vertical rain rates were transformed into vertical rain rates, following the rationale explained in section 5.1. For the four shallow POOZ samples (see Table 3, footnote d, and Table 4, footnote b) we report both the estimates taking into account the preservation rates estimated using (4) or assuming a 100% barite preservation.

5.3.1. Atlantic sector. [31] The estimates of export production vary between 1.8 and 25 g C m^{-2} yr^{-1} along the ANT X/6 transect (Table 3), and smallest variations are observed in the PFZ Zone (4–5.8 g C m^{-2} yr^{-1}). The accuracy of the export production estimates is affected by the accuracy of the ^{230}Th correction, which may not be particularly straightforward for the POOZ because of the following two reasons: (1) The POOZ is under the influence of the outflow of dissolved ^{230}Th enriched Weddell Sea water [*Walter*, 1998]. The dissolved ^{230}Th enrichment results from a low scavenging rate in the Weddell Sea due to low particle fluxes [*Rutgers van der Loeff and Berger*, 1983; *Walter et al.*, 1997]. Consequently, in the POOZ the vertical flux of ^{230}Th is higher than the production rate, potentially leading to an underestimation of export production by up to a factor of 2 (M. M. Rutgers van der Loeff, personal communication, 2000). (2) Correction of MAR according to the constant ^{230}Th flux model requires that redistributed particles are advected from an area characterized by a similar ^{230}Th rain rate, i.e., from an area with similar water column height [*François et al.*, 1993; R. François, personal communication, 2000]. If the

redistributed sediment was initially deposited in a shallower area before being transported to its final site of deposition, its lower excess ^{230}Th content will dilute the local excess. The error on the vertical flux ranges between 10 and 40% (R. François, personal communication, 2000) and would ultimately result in an underestimation of export production. Such a sediment supply from a shallow area has been reported for the region in vicinity of Maud Rise [*Abelmann and Gersonde*, 1991; *Van Bennekom et al.*, 1988]. Thus a rough seafloor topography (e.g., the presence of Antarctica-America Ridge) favors advective supply of ^{230}Th from adjacent shallower sites.

[32] We now compare our export production estimates deduced from sediment Baxs content with estimates based on other approaches, using data from the same ANT X/6 cruise or different cruises in the same region. From Table 5 it appears that all the water column proxies record highest export productions for the Polar Front.

1. From trapped Ba fluxes at the PF (station PF3; traps at 600 and 3200 m) and in the POOZ (station WS3; trap at 360 m), *Nürnberg* [1995] calculated export productions (at 100 m) of 5.6 g C m^{-2} yr^{-1} (PFZ) and 1.3 g C m^{-2} yr^{-1} (POOZ). After correcting these values for trapping efficiencies on the basis of annual ^{230}Th fluxes [*Walter*, 1998], the export production estimate for the PF site increases to 9.9–10.2 g C m^{-2} yr^{-1}.

2. *Rutgers van der Loeff et al.* [1997] observed a significant enhancement of the ^{234}Th deficit in the PFZ surface waters at 6°W (ANT X/6) during the bloom development, from which they deduced an export production of 3.6–9.6 g C m^{-2}. For the POOZ they observed a lower ^{234}Th-based export production of 1.8–3.6 g C m^{-2}.

3. Model results of the seasonal bloom development during the ANT X/6 cruise [*Lancelot et al.*, 2000] indicate export production for the PFZ ranges from 1 to 7.6 g C m^{-2} yr^{-1} and is 1.2 g C m^{-2} yr^{-1} for the POOZ.

4. For the same Atlantic transect (ANT X/6), export production was also calculated from mesopelagic organic carbon oxidation rates based on dissolved oxygen consumption rates or on the amount of mesopelagic particulate Baxs buildup since the onset of the growth season [*Dehairs et al.*, 1997]. The latter estimate should be smaller than the export production since it represents only a fraction (albeit large) of the downward carbon flux from the mixed surface layers. It appears for the PFZ that 2.7 g C m^{-2} yr^{-1} would be respired in the subsurface water layer between 200 and 400 m. This value reduces to 1.7 g C m^{-2} yr^{-1} for the POOZ and to 1.1 g C m^{-2} yr^{-1} for the SIZ.

[33] Although estimates based on the different proxies and approaches are quite variable, the results, in general, indicate that export production is at least 1.5 times higher in the PFZ compared to the POOZ (Table 5). It is important to note that export production values reported by *Frank et al.* [1996] and *François et al.* [1997], as obtained from dissolution-corrected, ^{230}Th-normalized sedimentary Baxs fluxes, are much higher for the POOZ (15–24 g C m^{-2} yr^{-1}) and are at least twice as high for the PFZ (5–10 g C m^{-2} yr^{-1}; Table 5). There is evidence that maximal export production occurs in the high opal flux belt of the Atlantic sector located south of the Polar Front [e.g., *Quéguiner et al.*, 1997], although it remains unclear as to what extent this massive opal deposition results from local high productivity, rather than from enhanced sediment focusing [*Rutgers van der Loeff et al.*, 1997]. For the POOZ our minimal estimates of export production are close to values based on water column proxies. This observation emphasizes that south of the Polar Front, barite preservation may be underestimated when using the Dymond et al. algorithm (equation (4)).

5.3.2. Indian sector. [34] In the Indian sector the mean export production estimate for the PFZ (4.6 g C m^{-2} yr^{-1}; one

value >20 g C m^{-2} yr^{-1} excluded; Table 4) is quite similar to the mean estimate for the Atlantic sector (4.9 g C m^{-2} yr^{-1}). For the POOZ the mean export production value is lower than the PFZ value and usually lower than the estimates for the Atlantic sector. *François et al.* [1997] reported an export production of 22 g C m^{-2} yr^{-1} for the Antarctic Zone of the Indian sector (Table 5). This estimate was based on dissolution-corrected, ^{230}Th-normalized Baxs flux of one surface sediment sample (MD84552) in the POOZ close to Kerguelen Island. Again, two processes may possibly contribute to an overestimation of export production: (1) The barite preservation rate may be higher than indicated by (4), and (2) the advective supply of excess ^{230}Th from sites with a shallower water column could dilute the ^{230}Th excess at the sampling site and lead to an overestimation of the Baxs flux. In the SIZ the two surface sediments also give a high export production of 11 and 27 g C m^{-2} yr^{-1}. The latter samples were collected in the eastern part of the study area, and we have no other data for direct comparison. Furthermore, the sampled location is characterized by intense winnowing (focusing factor <1; Table 4). The preservation rates, as deduced from (4), are thus minimum values, and the export production estimates are maximum values.

6. Conclusions

[35] The use of sediment Baxs content as a proxy for export production requires the conversion of the Baxs accumulation rates into vertical rain rates. This conversion in turn requires (1) an estimation of the degree of barite preservation from dissolution and (2) a correction for sedimentary reworking, mainly focusing.

1. Up to now, only the relationship between the degree of preservation of barite and the mass accumulation rate proposed by *Dymond et al.* [1992] has been available to correct for barite dissolution at the sediment-seawater interface. This correction takes into account the exposure time of sediment to undersaturated bottom waters. However, the observed relationship between sediment Baxs content and barite saturation index of bottom waters in the Atlantic sector suggests control also by the state of undersaturation in bottom waters.

Confronting our results with investigations on the saturation state of the water column with respect to barite has shown that correction for dissolution is widely justified, except maybe for shallow sediments (water depth <2500 m) located south of the Polar Front.

2. The excess ^{230}Th normalization of the Ba accumulation rate appears essential to correct for massive sediment focusing taking place in the Southern Ocean, but the correction has to be applied with caution because of the possible impact of boundary scavenging and focusing of shallower sediments less enriched in excess ^{230}Th.

[36] Export production estimates from sediment Baxs give similar values for the Polar Front Zone in the Atlantic and Indian sectors (4.9 and 4.6 g C m^{-2} yr^{-1}, respectively). In the permanently open ocean zone our estimates are closer to those deduced from water column proxies than previous estimates. This observation suggests that barite is in fact better preserved in the sediments of the permanently open ocean zone than suggested by the Dymond et al. algorithm.

References

Anderson, R. F., and A. Fleer, Determination of natural actinides and plutonium in marine particulate materiel, *Anal. Chem.*, *54*, 1142–1147, 1982.

Anderson, R. F., N. Kumar, R. A. Mortlock, P. N. Froelich, P. Kublik, B. D. Dittrich-Hannen, and M. Suter, Late Quaternary changes in productivity in the Southern Ocean, *J. Mar. Syst.*, *17*, 497–514, 1998.

Abelmann, A., and R. Gersonde, Biosiliceous particle flux in the Southern Ocean, *Mar. Chem.*, *35*, 503–536, 1991.

Bareille, G., Flux sédimentaires: Paléoproductivité et Paléocirculation de l'Océan Austral au cours des 150.000 dernières années, doctoral dissertation, 259 pp., Univ. de Bordeaux I, Talence, France, 1991.

Bareille, G., M. Labrachie, L. Labeyrie, J. J. Pichon, and J. L. Turon, Biogenic silica accumulation rate during the Holocene in the southeastern Indian Ocean, *Mar. Chem.*, *35*, 537–551, 1991.

Bareille, G., M. Labrachie, P. Bertrand, L. Labeyrie, G. Lavaux, and M. Dignan, Glacial-

interglacial changes in the accumulation rates of major biogenic components in southern Indian Ocean sediments, *J. Mar. Syst.*, *17*, 527–539, 1998.

Bathmann, U. V., R. Scharek, C. Klaas, C. D. Dubischar, and V. Smetacek, Spring development of phytoplankton biomass and composition in major water masses of the Atlantic sector of the Southern Ocean, *Deep Sea Res., Part II*, *44*, 51–67, 1997.

Bishop, J. K. B., The barite-opal-organic carbon association in oceanic particulate matter, *Nature*, *332*, 341–343, 1988.

Bishop, J. K. B., Regional extremes in particulate matter composition and flux: Effects on the chemistry of the ocean interior, in *Productivity of the Ocean: Present and Past*, edited by W. H. Berger, V. S. Smetacek, and G. Wefer, pp. 117–137, John Wiley, New York, 1989.

Broecker, W. S., and T. H. Peng, The cause of glacial to interglacial atmospheric CO_2 change: A polar alkalinity hypothesis, *Global Biogeochem. Cycles*, *3*, 215–239, 1989.

Brumsack, H. J., Geochemistry of recent TOC-

rich sediments from the Gulf of California and the Black Sea, *Geol. Rundsch.*, *78*, 851–882, 1989.

Cardinal, D., N. Fagel, L. André, and F. Dehairs, Ba repartition in surface sediment and trap material: A sequential leaching approach, *J. Conf. Abstr. EUG X*, *4*, 425, 1999.

Charles, C. D., P. N. Froelich, M. A. Zibello, R. A. Mortlock, and J. J. Morely, Biogenic opal in Southern Ocean sediments, over the last 450,000 years: Implications for surface water chemistry and circulation, *Paleoceanography*, *6*, 697–728, 1991.

Church, T. M., Marine barite, in *Marine Minerals*, edited by R. G. Burns, *Rev. Mineral.*, *6*, 175–209, 1979.

Dehairs, F., R. Chesselet, and J. Jedwab, Discrete suspended particles of barite and the barium cycle in the open ocean, *Earth Planet. Sci. Lett.*, *49*, 529–550, 1980.

Dehairs, F., N. Stroobants, and L. Goeyens, Suspended barite as a tracer of biological activity in the Southern Ocean, *Mar. Chem.*, *35*, 399–410, 1991.

Dehairs, F., D. Shopova, S. Ober, C. Veth, and L. Goeyens, Particulate barium stocks and oxygen consumption in the Southern Ocean mesopelagic water column during spring and early summer: Relationship with export production, *Deep Sea Res., Part II*, *44*, 497–516, 1997.

Dezileau, L., G. Bareille, J. L. Reyss, F. Lemoine, and L. Labeyrie, Evidence for strong sediment redistribution by bottom currents along the Southeastern Indian Ridge, *Deep Sea Res., Part I*, *47*, 1899–1936, 2000.

Dymond, J., E. Suess, and M. Lyle, Barium in deep-sea sediment: A geochemical proxy for paleoproductivity, *Paleoceanography*, *7*, 163–181, 1992.

Dymond, J., R. Collier, J. McManus, S. Honjo, and S. Manganini, Can the aluminum and titanium contents of ocean sediments be used to determine the paleoproductivity of the oceans?, *Paleoceanography*, *12*, 586–593, 1997.

Fagel, N., L. André, and F. Dehairs, Advective excess Ba transport as shown from sediment and trap geochemical signatures, *Geochim. Cosmochim. Acta*, *16*, 2353–2367, 1999.

François, R., M. A. Altabet, and L. H. Burckle, Glacial to interglacial changes in surface nitrate utilization in the Indian sector of the Southern Ocean as recorded by sediment $\delta^{15}N$, *Paleoceanography*, *7*, 589–606, 1992.

François, R., M. P. Bacon, M. A. Altabet, and L. Labeyrie, Glacial/interglacial changes in sediment rain rate in the SW Indian sector of subantarctic waters as recorded by ^{230}Th, ^{231}Pa, U, and $\delta^{15}N$, *Paleoceanography*, *8*, 611–629, 1993.

François, R., S. Honjo, S. Manganini, and G. E. Ravizza, Biogenic barium fluxes to the deep sea: Implications for paleoproductivity reconstruction, *Global Biogeochem. Cycles*, *9*, 289–303, 1995.

François, R., M. A. Altabet, F. E. Yu, D. M. Sigman, M. P. Bacon, M. Frank, G. Bohrmann, G. Bareille, and L. Labeyrie, Contribution of Southern Ocean surface-water stratification to low atmospheric CO_2 concentrations during the last glacial period, *Nature*, *389*, 929–935, 1997.

Frank, M., Reconstruction of late Quaternary environmental conditions applying the natural radionuclides ^{230}Th, ^{10}Be, ^{231}Pa and ^{238}U: A study of deep-sea sediments from the eastern sector of the Antarctic Circumpolar Current system, *Ber. Polarforsch.*, *186*, 136 pp., 1996.

Frank, M., R. Gersonde, M. Rutgers van der Loeff, G. Kuhn, and A. Mangini, Late Quaternary sediment dating and quantification of lateral sediment redistribution applying $^{230}Th_{ex}$: A study from the eastern Atlantic sector of the Southern Ocean, *Geol. Rundsch.*, *85*, 554–566, 1996.

Frank, M., R. Gersonde, M. Rutgers van der Loeff, G. Bohrmann, C. Nürnberg, P. W. Kubik, M. Suter, and A. Mangini, Similar glacial and interglacial export productivity in the Atlantic sector of the Southern Ocean: Multiproxy evidence and implications for glacial atmospheric CO_2, *Paleoceanography*, *15*, 642–658, 2000.

Gingele, F., and A. Dahmke, Discrete barite particles and barium as tracers of paleoproductivity in South Atlantic sediments, *Paleoceanography*, *9*, 151–168, 1994.

Gingele, F., M. Zabel, S. Kasten, W. J. Bonn, and C. C. Nürnberg, Biogenic barium as a proxy for paleoproductivity: Methods and limitations of application, in *Use of Proxies in Paleoceanography: Examples From the South Atlantic*, edited by G. Fischer and G. Wefer, pp. 345–364, Springer-Verlag, New York, 1999.

Goldberg, E. D., and G. O. S. Arrhenius, Chemistry of Pacific pelagic sediments, *Geochim. Cosmochim. Acta*, *13*, 153–212, 1958.

Keir, R. S., Reconstructing the ocean carbon system variation during the last 150,000 years according to the Antarctic nutrient hypothesis, *Paleoceanography*, *5*, 253–276, 1990.

Knox, F., and M. B. McElroy, Changes in atmospheric CO_2: Influence of marine biota at high latitudes, *J. Geophys. Res.*, *89*, 4629–4637, 1984.

Kumar, N., Trace metals and natural radionuclides as tracers of ocean productivity, Ph.D. thesis, 317 pp., Columbia Univ., New York, 1994.

Kumar, N., R. Gwiazda, R. F. Anderson, and P. N. Froelich, $^{231}Pa/^{230}Th$ ratios in sediments as a proxy for past changes in Southern Ocean productivity, *Nature*, *362*, 45–48, 1993.

Lancelot, C., E. Hannon, S. Becquevort, C. Veth, and H. J. De Baar, Modeling phytoplankton blooms and carbon export production in the Southern Ocean: Dominant controls by light and iron in the Atlantic sector in Austral spring 1992, *Deep Sea Res., Part I*, *47*, 1621–1662, 2000.

Martin, J. H., Glacial-interglacial CO_2 change: The iron hypothesis, *Paleoceanography*, *5*, 1–13, 1990.

Martin, J. H., S. E. Fitzwater, and R. M. Gordon, Iron deficiency limits phytoplankton growth in Antarctic waters, *Global Biogeochem. Cycles*, *4*, 5–12, 1990.

McManus, J., W. H. Berelson, G. P. Klinkhammer, T. E. Kilgore, and D. E. Hammond, Remobilization of barium in continental margin sediments, *Geochim. Cosmochim. Acta*, *58*, 4899–4907, 1994.

McManus, J., et al., Geochemistry of barium in marine sediments: Implications for its use as a paleoproxy, *Geochim. Cosmochim. Acta*, *62*, 3453–3473, 1998.

McManus, J., W. M. Berelson, D. E. Hammond, and G. P. Klinkhammer, Barium cycling in the North Pacific: Implications for the utility of Ba as a paleoproductivity and paleoalkalinity proxy, *Paleoceanography*, *14*, 53–61, 1999.

Monnin, C., C. Jeandel, T. Cattaldo, and F. Dehairs, The marine barite saturation state of the world's oceans, *Mar. Chem.*, *65*, 253–261, 1999.

Moore, J. K., M. R. Abbott, J. R. Richman, and D. Nelson, The Southern Ocean at the Last Glacial Maximum: A strong sink for atmospheric carbon dioxide, *Global Biogeochem. Cycles*, *14*, 455–475, 2000.

Murray, R. W., and M. Leinen, Scavenged excess aluminum and its relationship to bulk titanium in biogenic sediment from the central equatorial Pacific Ocean, *Geochim. Cosmochim. Acta*, *60*, 3869–3878, 1996.

Navez, J., Méthodes d'analyse des éléments majeurs dans les roches silicatées basée sur la spectrométrie d'émission dans un plasma à couplage inductif, *Dep. Geol. Min. Rapp. Ann. 1983–1984*, pp. 87–90, Mus. R. Afr. Cent., Tervuren, Belgium, 1985.

Nürnberg, C. C., Bariumfluss und sedimentation in der südlichen Südatlantik-Hinweise auf produktivitätsänderungen im Quartär, doctoral dissertation, 105 pp., Christian-Albrechts-Univ. zu Kiel, Kiel, Germany, 1995.

Nürnberg, C. C., G. Bohrmann, and M. Schluter, Barium accumulation in the Atlantic sector of the Southern Ocean: Results from 190,000-year records, *Paleoceanography*, *12*, 594–603, 1997.

Orsi, A. H., T. Whitworth, and W. D. Nowlin, On the meridional extent and fronts of the Antarctic Circumpolar Current, *Deep Sea Res., Part I*, *42*, 641–673, 1995.

Paytan, A., M. Kastner, E. E. Martin, J. D. Macdougall, and T. Herbert, Marine barite as a monitor of seawater strontium isotope composition, *Nature*, *366*, 445–449, 1993.

Paytan, A., M. Kastner, and F. P. Chavez, Glacial to interglacial fluctuations in productivity in the equatorial Pacific as indicated by marine barite, *Science*, *274*, 1355–1357, 1996.

Peterson, R. G., and L. Stramma, Upper-level circulation in the South Atlantic Ocean, *Prog. Oceanogr.*, *26*, 1–73, 1991.

Quéguiner, B., P. Tréguer, I. Peeke, and R. Scharek, Biogeochemical dynamics and the silicon cycle in the Atlantic sector of the Southern Ocean during austral spring 1992, *Deep Sea Res., Part II*, *44*, 69–89, 1997.

Rutgers van der Loeff, M. M., and G. W. Berger, Scavenging of ^{230}Th and ^{231}Pa near the Antarctic Polar Front in the South Atlantic, *Deep Sea Res., Part I*, *40*, 339–357, 1983.

Rutgers van der Loeff, M. M., J. Friedrich, and U. V. Bathmann, Carbon export during the spring bloom at the Antarctic Polar Front, determined with the natural tracer ^{234}Th, *Deep Sea Res., Part II*, *44*, 457–478, 1997.

Sarmiento, J. L., and J. R. Toggweiler, A new model for the role of the oceans in determining atmospheric pCO$_2$, *Nature*, *308*, 621–626, 1984.

Sarnthein, M., K. Winn, J. C. Duplessy, and M. R. Fontugne, Global variations of surface ocean productivity in low and mid latitudes: Influence on CO_2 reservoirs of the deep ocean and atmosphere during the last 21,000 years, *Paleoceanography*, *3*, 361–399, 1988.

Schmitz, B., Barium, equatorial high productivity, and the northward wandering of the Indian continent, *Paleoceanography*, *2*, 63–77, 1987.

Schroeder, J. O., R. W. Murray, M. Leinen, R. C. Pflaum, and T. R. Janecek, Barium in equatorial Pacific carbonate sediment: Terrigenous, oxide and biogenic associations, *Paleoceanography*, *12*, 125–146, 1997.

Shemesh, A., S. A. Macko, C. D. Charles, and G. H. Rau, Isotopic evidence for reduced productivity in the glacial southern Ocean, *Science*, *262*, 407–410, 1993.

Shimmield, G. B., Can sediment geochemistry record changes in coastal upwelling palaeoproductivity? Evidence from northwest Africa and the Arabian Sea, in *Upwelling Systems Since the Early Miocene*, edited by C. W. Prell and K. Emeis, *Geol. Soc. Spec. Publ.*, *64*, 29–46, 1992.

Shimmield, G., S. Derrick, A. Mackensen, H. Grobe, and C. Pudsey, The history of barium, biogenic silica and organic carbon accumulation in the Weddell Sea and Antarctic Ocean over the last 150,000 years, in *Carbon Cycling in the Glacial Ocean: Constraints on the Ocean's Role in Global Change*, NATO ASI Ser., Ser. I, vol. X, edited by R. Zahn et al., pp. 555–574, Springer-Verlag, New York, 1994.

Siegenthaler, U., and T. Wenk, Rapid atmo-

spheric CO_2 variations and ocean circulation, *Nature*, *308*, 624–626, 1984.

Smetacek, V., H. J. W. DeBaar, U. V. Bathmann, K. Lochte, and M. M. Rutgers van der Loeff, Ecology and biogeochemistry of the Antarctic Circumpolar Current during austral spring: A summary of Southern Ocean JGOFS cruise ANT X/6 of R/V Polarstern, *Deep Sea Res., Part II*, *44*, 1–21, 1997.

Stephens, B. B., and R. F. Keeling, The influence of Antarctic sea ice on glacial-interglacial CO_2 variations, *Nature*, *404*, 171–174, 2000.

Stroobants, N., F. Dehairs, L. Goeyens, N. Vanderheijden, and R. Van Grieken, Barite formation in the Southern Ocean water column, *Mar. Chem.*, *35*, 411–422, 1991.

Taylor, S. R., and S. M. McLennan, *The Continental Crust: Its Composition and Evolution*, Blackwell, Malden, Mass., 1985.

Van Bennekom, A. J., G. W. Berger, S. J. Van der Gaast, and R. T. P. De Vries, Primary productivity and the silica cycle in the southern ocean (Atlantic sector), *Paleogeogr. Paleoclimatol. Paleoecol.*, *67*, 19–30, 1988.

Veth, C., I. Peeken, and R. Scharek, Physical anatomy of fronts and surface waters in the ACC near the 6°W meridian during austral spring 1992, *Deep Sea Res., Part II*, *44*, 23–49, 1997.

Von Breymann, M. T., K. C. Emeis, E. Suess, Water depth and diagenetic constraints on the use of barium as a paleoproductivity indicator, in *Upwelling Systems: Evolution Since the Early Miocene*, edited by C. P. Summerhayes, W. L. Prell, and K. C. Emeis, *Geol. Soc. Spec. Publ., 64*, 273–284, 1992.

Walter, H.-J., Scavenging of [231]Pa and [230]Th in the South Atlantic: Implications for the use of the [231]Pa/[230]Th ratio as a paleoproductivity proxy, *Rep. 282*, Alfred Wegener Inst., Bremerhaven, Germany, 1998.

Walter, H.-J., M. M. Rutgers van der Loeff, and H. Holtzen, Enhanced scavenging of [231]Pa relative to [230]Th in the South Atlantic south of the Polar Front: Implications for the use of [231]Pa/[230]Th ratio as a paleoproductivity proxy, *Earth Planet. Sci. Lett.*, *149*, 85–100, 1997.

Yarincik, K. M., R. W. Murray, and L. C. Peterson, Climatically controlled eolian and hemipelagic deposition in the Cariaco Basin, Venezuela, over the past 578,000 years: Results from Al/Ti and K/Al, *Paleoceanography*, *15*, 210–228, 2000.

L. André, Mineralogy and Geochemistry Department, Royal Museum for Central Africa, 3080 Tervuren, Belgium.

G. Bareille, Laboratoire de Chimie Analytique Bio-organique et Environnement (LCABIE), UMR-CNRS 5034, Université de Pau et des Pays de l'Adour, hélioparc Pau Pyrénées, 2 avenue du Président Angot, 64053 Pau cedex 9, France.

F. Dehairs, Analytical Chemistry Department, Vrije Universiteit Brussel, 1050 Brussels, Belgium.

N. Fagel, Clay Mineralogy Department, Université de Liège, Allée du 6 août, B18 Sart-Tilman, Liège, Belgium. (nathalie.fagel@ulg.ac.be)

C. Monnin, Laboratory of Geochemistry, University Paul Sabatier, 31400 Toulouse, France.